R-13-39

Recommendation of rock matrix effective diffusivities for SR-PSU

Based on formation factor logging in situ by electrical methods in KFR102B and KFR105

Martin Löfgren, Niressa AB

April 2014

Svensk Kärnbränslehantering AB
Swedish Nuclear Fuel
and Waste Management Co

Box 250, SE-101 24 Stockholm
Phone +46 8 459 84 00

ISSN 1402-3091
SKB R-13-39
ID 1399532

Recommendation of rock matrix effective diffusivities for SR-PSU

Based on formation factor logging in situ by electrical methods in KFR102B and KFR105

Martin Löfgren, Niressa AB

April 2014

Keywords: SFR, SR-PSU, In situ, Formation factor, Rock resistivity, Effective diffusivity.

Abstract

This report recommends rock matrix effective diffusivities of the SFR host rock, for use in the safety assessment SR-PSU. The recommendations are primarily based on interpretations of the in situ formation factor of the rock surrounding the boreholes KFR105 and KFR102B at the SFR site in Forsmark, Sweden. Underlying data were obtained in site investigation SFR, and are used in a methodology called "formation factor logging in situ by electrical methods". When interpreting the data, corrections for surface conduction have been made in the same way as done in SR-Site.

For KFR105, the 264 obtained in situ rock matrix formation factors range from 2.9×10^{-5} to 2.5×10^{-3}, with an arithmetic mean of 1.1×10^{-4}. The 1,673 obtained in situ fractured rock formation factors range from 2.3×10^{-5} to 2.5×10^{-3}, with an arithmetic mean of 2.2×10^{-4}. The obtained formation factor distributions correspond fairly well with the log-normal distribution. The mean values and standard deviations of the fitted $\log_{10}$-normal distributions are –4.07 and 0.29, and –3.84 and 0.38, for the in situ rock matrix and fractured rock formation factor, respectively.

For KFR102B, the 86 obtained in situ rock matrix formation factors range from 9.8×10^{-6} to 2.3×10^{-4}, with an arithmetic mean of 4.7×10^{-5}. The 901 obtained in situ fractured rock formation factors range from 9.4×10^{-6} to 1.3×10^{-3}, with an arithmetic mean of 1.1×10^{-4}. The distributions of the formation factors are fairly well described by the log-normal distribution. The mean values and standard deviations of the fitted $\log_{10}$-normal distributions are –4.45 and 0.33, and –4.17 and 0.40, for the in situ rock matrix and fractured rock formation factor, respectively.

When writing this report, no matrix fluid measurements on drill core samples had been made at the SFR site. Therefore, the estimate of the electrical conductivity of the matrix pore water had to be based solely on data obtained on freely flowing groundwater, as well as interpretations made in the hydrogeochemical part of the SFR site descriptive modelling.

It is simplistically assumed that the arithmetic mean of all data obtained in the two boreholes corresponds to a representative flowpath averaged formation factor; for use in subsequent solute transport modelling. This arithmetic mean of the in situ rock matrix formation factor is 9.4×10^{-5}.

Concerning the effective diffusivity, many of the recommendations given in SR-Site are adapted. Similar uncertainty distributions are assumed for the effective diffusivity, by way of using the log-normal distribution having the same standard deviation as in SR-Site. However, the distributions are shifted to accommodate the arithmetic mean of SFR data. For cations and non-charged species, the recommended distribution parameters of $\log_{10}(D_e)$ are $\mu = -13.0$ and $\sigma = 0.25$. For anions, experiencing anion exclusion effects, the corresponding distribution parameters are $\mu = -13.5$ and $\sigma = 0.25$.

The fact that the two investigated boreholes at the SFR site have very different inclinations may contribute to differences in their sets of formation factors, perhaps due to minor anisotropy effects. Compared to the host rock for the planned KBS-3 repository at Forsmark, formation factors are on average a factor of about four to five times larger at the SFR site. This is not unexpected, as the investigated rock at the SFR site is shallower and sustains less stress from the overburden.

Contents

1 Introduction

This report recommends rock matrix effective diffusivities D_e (m^2/s) for the crystalline host rock surrounding SFR, as well as its planned extension. These data are required for radionuclide (and possibly other solute) transport modelling in the geological barrier in the safety assessment SR-PSU. In previous safety assessments for SFR (e.g. Thomson et al. 2008), generic effective diffusivities have been used due to a lack of SFR site specific data. Furthermore, no effective diffusivity is suggested in the site descriptive modelling for SFR. To amend this lack of data, in situ measurements from site investigation SFR have been revisited. Based on these measurements, in situ formation factors of the rock surrounding boreholes KFR105 and KFR102B have been obtained.

This has been done by formation factor logging in situ by electrical methods, which is a methodology that was introduced in the Forsmark and Oskarshamn site investigations for a KBS-3 repository. The governing texts describing this methodology are Löfgren and Neretnieks (2005a) and SKB (2010a, Section 6.8), with supporting texts such as Crawford (2008, Appendix H). The minor modifications made are fully documented in this present report. The reasons for choosing boreholes KFR105 and KFR102B, out of the existing core drill boreholes at the SFR site, are the following

- There exist background data both on the rock resistivity and on the groundwater electrical conductivity, as prescribed by the used methodology.
- In a preliminary study, also including a few other boreholes, these two boreholes were chosen as they display sufficiently large non-fractured sections. This facilitates estimations of the rock matrix formation factor.
- One of the boreholes, KFR102B, is drilled from the surface. In the Forsmark and Oskarshamn site investigations for the KBS-3 repository, no shallow in situ formation factors were obtained. Therefore, the shallow part of KFR102B provides unprecedented data on the in situ formation factor in the upper 50 metres of the rock mass (although the shallow rock is heavily fractured).
- The other borehole, KFR105, is drilled from the SFR underground facility in a direction so that it intersects the rock mass intended to host the extended SFR repository.

Figure 1-1 shows the SFR site and the location of some of the different boreholes, including the core drilled boreholes KFR105 and KFR102B. Borehole KFR105 is 306.81 m long, is drilled from a SFR tunnel at the elevation –106.82 m (RHB70), and extends down to an elevation of –156.63 m (Nilsson G 2009). Borehole KFR102B is 180.08 m long, is drilled from ground surface, and extends down to the elevation –142.88 m (Nilsson and Ullberg 2009). As borehole KFR105 is almost horizontal (dip approximately 10°), measurements in this borehole may catch anisotropy effects of the rock matrix that are not seen in boreholes drilled from the surface, which generally have a more vertical direction. By comparing data from borehole KFR105 (almost horizontal) with data from KFR102B (almost vertical) anisotropy effects can be investigated.

Other contractors performed the fieldwork, as documented in background reports. The interpretation of in situ data and compilation of formation factor logs and distributions were performed by Niressa AB in Stockholm, Sweden.

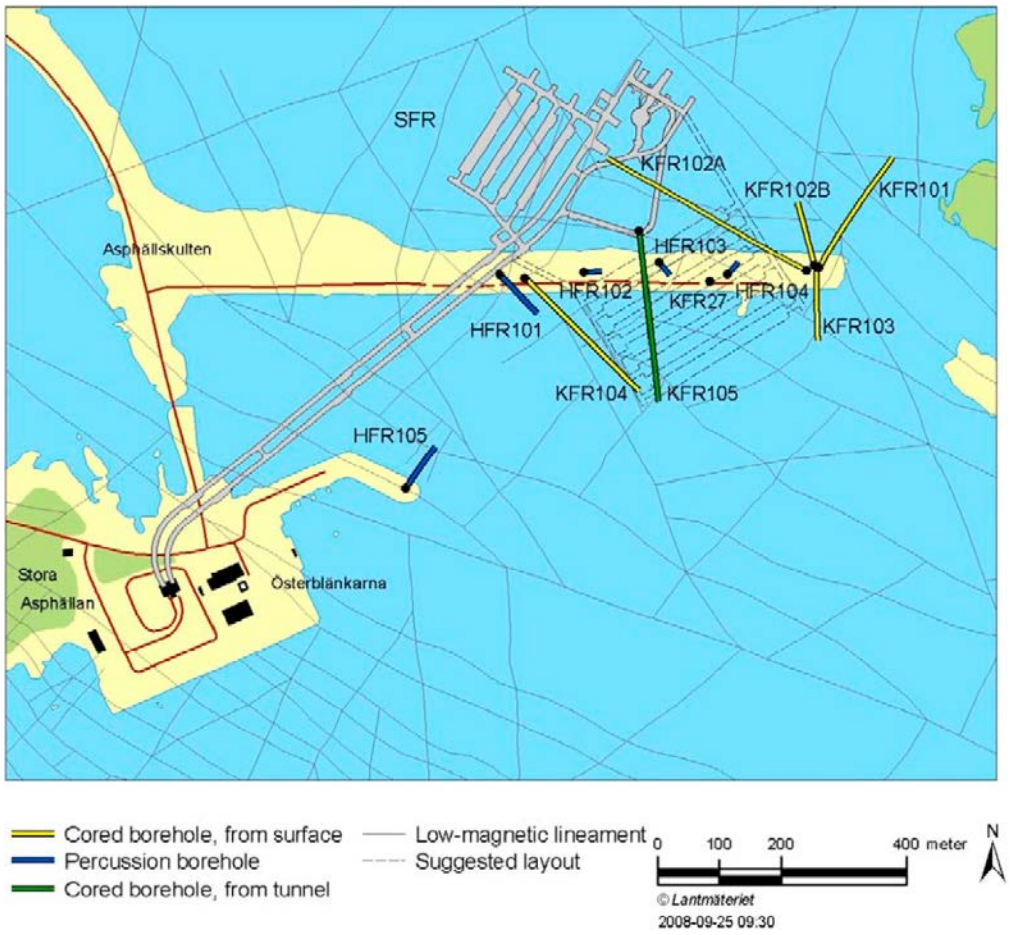

Figure 1-1. *General overview of the SFR site. Borehole KFR105 is marked by green and borehole KFR102B is located on the right. Reproduced from Kristiansson and Väisäsvaara (2008, Figure 1-1).*

2 Objective and scope

The formation factor is an important parameter that may be used directly, or as converted to the effective diffusivity, in safety assessment calculation of solute transport in fractured crystalline rock.

A main objective of this work is to obtain formation factors of the rock mass surrounding the boreholes KFR105 and KFR102B, situated at the SFR site in Forsmark, Sweden. This has been achieved by performing formation factor logging in situ by electrical methods. The in situ method gives a great number of formation factors obtained under more natural conditions than in the laboratory. To obtain the in situ formation factor, results from previous measurements were used. In obtaining the formation factor, corrections for surface conduction were made in agreement with the methodology used in the SR-Site safety assessment (SKB 2010a, Section 6.8). The effort of obtaining in situ formation factors is reported in Chapters 3 to 5. In order to facilitate direct comparisons with a series of site investigation reports documenting the in situ formation factor logging at the Forsmark and Oskarshamn sites (Löfgren and Neretnieks 2005a, b, Löfgren 2007, etc.), the outline of Chapters 3 to 5 of this report adheres to a template previously defined by SKB.

A second main objective is to recommend effective diffusivities for use in the safety assessment SR-PSU, especially for radionuclide transport modelling. These data should be delivered as probability density functions, as well as corresponding to flowpath averaged effective diffusivities. In doing this, the recommendations given in the SR-Site data report (SKB 2010a, Section 6.8) are followed. This effort, together with the recommended set of effective diffusivities, is reported in Chapter 6.

3 Equipment

As part of obtaining in situ formation factors by electrical methods (cf. Section 4.1), the rock resistivity as well as the electrical conductivity (EC) of the rock matrix pore fluid are needed. When determining what data points may have been affected by flowing water in hydraulically conductive fractures, as well as by free water in open fractures, data from flow loggings as well as the drill core mapping are used. These methods are summarised below.

3.1 Rock resistivity loggings

The resistivity of the rock surrounding the boreholes KFR105 (Nielsen and Ringgaard 2009a) and KFR102B (Nielsen and Ringgaard 2009b) was logged using the focused rock resistivity tool Century 9072. The tool emits an alternating current perpendicular to the borehole axis from a main current electrode. The shape of the current field is controlled by electric fields emitted by guard electrodes. By using a focused tool, the disturbance from the borehole is minimised. The quantitative measuring range of the Century 9072 tool is 0–50,000 ohm.m according to the manufacturer. Comparative measurements performed by SKB suggest an even larger quantitative measuring range (Löfgren and Neretnieks 2005b, Figure 4-13).

3.2 Groundwater electrical conductivity measurements

The EC (electrical conductivity) of the borehole fluid in KFR105 (Väisäsvaara 2009) and KFR102B (Kristiansson and Väisäsvaara 2008) was logged using the Posiva difference flow meter. The tool is shown in Figure 3-1.

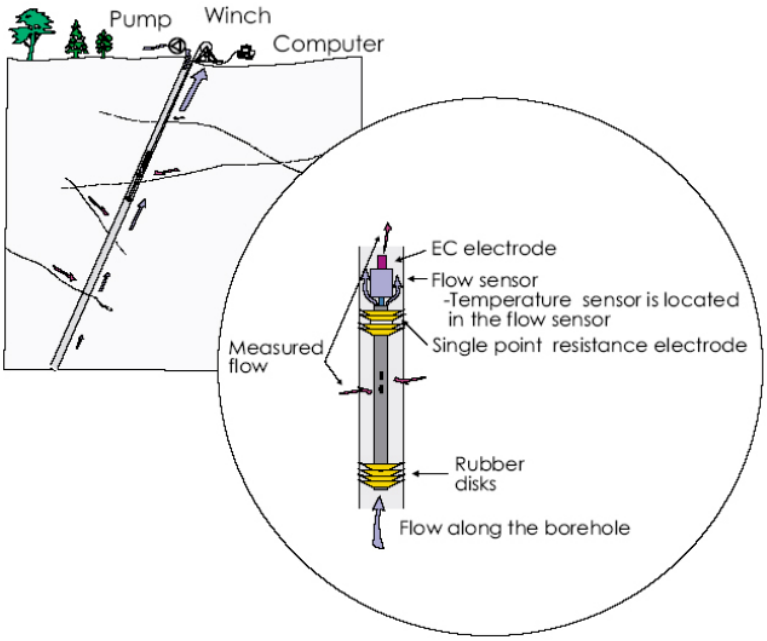

Figure 3-1. *Schematics of the Posiva difference flow meter. Reproduced from Kristiansson and Väisäsvaara (2008, Figure 3-1).*

When logging the EC of the borehole fluid, the lower rubber disks of the tool are not used. During the measurements, a drawdown can either be applied or not. Measurements were carried out before and after, or at, extensive pumping in the boreholes.

When using both the upper and the lower rubber disks, a section around a specific fracture can be packed off. By applying a drawdown at the surface, groundwater can thus be extracted from specific fractures. This is done in fracture-specific EC measurements. By also measuring the groundwater flow out of the fracture, it is calculated how long time it will take to fill up the packed off borehole section three times. During this time the EC is measured and a transient EC curve is obtained. After this time it is assumed that the measured EC in unaffected by the borehole fluid initially filling the section and is representative of the groundwater flowing out of the fracture. The measurements may be disturbed by leakage of borehole fluid into the packed off section and development of gas from species dissolved in the groundwater. Interpretations of transient EC curves are discussed in Löfgren and Neretnieks (2005a). The quantitative measuring range of the EC electrode of the Posiva difference flow meter is 0.02–11 S/m.

The EC, among other entities, of the groundwater coming from fractures in larger borehole sections is measured as a part of the hydrochemical characterisation using the Chemmac equipment. A section is packed off and by (normally) using a drawdown, groundwater is extracted from fractures within the section and brought to the surface for chemical analysis. For some parameters, including the EC, measurements are also made online in the borehole. Hydrochemical characterisation was performed in KFR105 (Lindquist and Nilsson 2010).

3.3 Difference flow loggings

By using the Posiva difference flow meter, water-conducting fractures can be located. The tool, shown in Figure 3-1, has a flow sensor and the flow from fractures in packed off sections can be measured. When performing these measurements, both the upper and the lower rubber disks are used. Measurements can be carried out both with and without applying a drawdown. The quantitative measuring range of the flow sensor is 0.1–5,000 ml/min. Difference flow loggings were performed in KFR105 (Väisäsvaara 2009) and KFR102B (Kristiansson and Väisäsvaara 2008).

3.4 Boremap loggings

The drill cores of KFR105 (Winell 2009) and KFR102B (Döse et al. 2009) were logged together with a simultaneous study of video images of the borehole wall. This is called Boremap logging.

In the core log, fractures parting the core are recorded. Fractures parting the core that have not been induced during the drilling or core handling are called broken fractures. An interpretation is made for each broken fracture whether it is open or sealed in situ. In this present report, this interpretation has been used. This is a modification of the methodology compared to previous reports describing formation factor logging in situ by electrical methods; where all broken fractures are treated as potentially open (e.g. Löfgren 2007, Section 3.4).

4 Execution

4.1 Theory

4.1.1 The formation factor

The theory applied for obtaining formation factors by electrical methods is described in SKB (2010a, Section 6.8) and references therein. The formation factor is the ratio between the diffusivity of the rock matrix to that of free pore water. If the species diffusing through the porous system is much smaller than the characteristic length of the pores and no interactions occur between the mineral surfaces and the species, the formation factor is only a geometric factor that is defined by the transport porosity, the tortuosity and the constrictivity of the porous system:

$$F_f = \frac{D_e}{D_w} = \varepsilon_t \frac{\delta}{\tau^2}$$ Equation 4-1

where F_f (–) is the formation factor, D_e (m^2/s) is the effective diffusivity of the rock matrix, D_w (m^2/s) is the diffusivity in the free pore water, ε_t (–) is the transport porosity, τ(–) is the tortuosity, and δ (–) is the constrictivity. When obtaining the formation factor with electrical methods, the Einstein relation between diffusivity and ionic mobility is used:

$$D = \frac{\mu RT}{zF}$$ Equation 4-2

where D (m^2/s) is the diffusivity, μ (m^2/V×s) is the ionic mobility, z (–) the charge number and R (J/mol×K), T (K) and F (C/mol), are the gas constant, temperature, and Faraday constant, respectively. By extrapolating the Einstein relation it can be assumed that the formation factor also is given by the ratio of the pore water resistivity to the resistivity of the saturated porous medium, if comprised of an inert matrix:

$$F_f = \frac{\rho_w}{\rho_{r,IM}}$$ Equation 4-3

where ρ_w (ohm.m) is the pore water resistivity and $\rho_{w,IM}$ (ohm.m) is the resistivity of the saturated rock, if having an inert matrix.

In crystalline rock the mineral surfaces are normally negatively charged, and therefore not inert. As the negative charge often is greater than what can be balanced by cations specifically adsorbed on the mineral surfaces, an electrical double layer with an excess of mobile cations will form at the pore wall. If an electrical potential gradient is placed over the rock, the excess cations in the electrical double layer will move. This process is called surface conduction and this additional conduction needs to be accounted for when obtaining the formation factor of rock, especially if saturated with a pore water of low ionic strength. As the rock matrix is not inert and interacts with the current bearing ions of the pore water, the ratio of the pore water resistivity and rock resistivity is the apparent formation factor F_f^{app} (–):

$$F_f{}^{app} = \frac{\rho_w}{\rho_r}$$ Equation 4-4

where ρ_r (ohm.m) is the resistivity of the saturated rock that can easily be obtained by standard geophysical methods.

To estimate the formation factor from rock resistivity data, corrections needs to be made for the contribution of surface conduction. For details on doing this, please turn to the SR-Site data report (SKB 2010a, Section 6.8). By using the same correction as done in SR-Site, the formation factor is obtained from the apparent formation factor by applying the following equation:

$$F_f = F_f{}^{app} - \frac{0.0012 \cdot F_f{}^{0.415}}{\kappa_w}$$ Equation 4-5

Where κ_w (S/m) is the electrical conductivity of the pore water, which is the reciprocal to the pore water electrical resistivity.

In a document (SKBdoc 1417017) recently provided by SKB to the Swedish Radiation Safety Authority, SSM, artefacts associated with formation factor measurements by electrical methods are discussed. The perhaps most prominent artefact that was identified originates in the fact that alternating current is used in the in situ measurements, as opposed to using direct current. Hence, two types of current conduction contribute in the saturated rock; electrolytic and dielectric conduction. While the Einstein relation should be suited for electrolytic conduction, the current contribution from dielectric conduction is regarded as an artefact that should be avoided, corrected for, or at least be bounded in magnitude. When comparing electrical measurements made on rock samples in the laboratory, at frequencies relevant for the in situ tool (Löfgren et al. 2009, Vecernik et al. 2012), it is indicated that the discrepancy of the current conduction when using alternating versus direct current is bounded by a factor of less than two, as long as the pore water composition is brackish or saline.

4.1.2 Fractures in situ

In situ rock resistivity measurements are highly disturbed by free water in open fractures. The electrical current sent out from the downhole tool in front of an open fracture will be propagated both in the porous system of the rock matrix and in the free water in the open fracture. Due to the low formation factor of the rock matrix, current may be preferentially propagated in a fracture intersecting the borehole if its aperture is on the order of 10^{-5} m or more. It should be noted that it is of no consequence for the measurements whether the open fracture contains stagnant or flowing water.

Two types of fractures are mapped in Boremap; broken and unbroken. Broken fractures are those that split the core, while unbroken fractures do not split the core. Broken fractures are interpreted to have been open or sealed in situ (e.g. Döse et al. 2009). In previous reports presenting formation factor logging in situ by electrical methods (e.g. Löfgren 2007), it has been assumed that all broken fractures may impact the rock resistivity log. However, it is known that sealed fractures have little impact on the rock resistivity, as they do not contain "free" water at a significantly larger fraction than the surrounding rock matrix. Therefore, in this present report the Boremap interpretation has been used and only fractures interpreted as open are assumed to impact the rock resistivity log. This implicitly means that it is assumed that the uncertainty evoked in interpreting broken fractures as open or sealed is relatively small. If interpreting naturally open fractures as sealed, and not discarding the corresponding resistivity data, this may locally give rise to unreasonably high rock matrix formation factors (see below).

4.1.3 Rock matrix and fractured rock formation factor

In this report the rock resistivity is used to obtain formation factors of the rock surrounding the borehole. The obtained formation factors may later be used in models for solute and radionuclide transport in fractured crystalline rock. Different conceptual approaches may be used in these models. Therefore this report aims to deliver formation factors that are defined in two different ways. The first is the "rock matrix formation factor", denoted by F_f^{rm} (–). This formation factor is representative of the solid, non-fractured, rock matrix, which is in line with what is traditionally associated with the formation factor. The other one is the "fractured rock formation factor", denoted by F_f^{fr} (–), which represents the diffusive properties of a larger rock mass, where fractures and voids holding stagnant water is included in the porous system of the rock matrix. Further information on the definition of the two formation factors can be found in Löfgren and Neretnieks (2005a).

The rock matrix formation factor is obtained from rock matrix resistivity data. When obtaining the rock matrix resistivity log from the in situ measurements, all resistivity data that may have been affected by open fractures have to be discarded. With present methods one cannot with certainty separate open fractures with a significant aperture from open fractures with an insignificant aperture in the interpretation of the core logging. It should be mentioned that there is an attempt to assess the fracture aperture in the interpretation of the core logging. However, this is done on a millimetre scale. Fractures may be significant even if they only have apertures some tens of micrometers.

By investigating the rock resistivity log at a fracture, one can draw conclusions concerning the fracture aperture. However, for formation factor logging by electrical methods this is not an independent method and cannot be used. Therefore, all interpreted open fractures have to be considered as having a significant aperture and all resistivities obtained close to an open fracture detected in the core logging are sorted out. By examining the resistivity logs obtained by the Century 9072 tool, it has been found that resistivity values obtained within 0.5 m from an open fracture generally should be discarded. This distance includes a safety margin of 0.1–0.2 m.

The fractured rock formation factor is obtained from fractured rock resistivity data. When obtaining the fractured rock resistivity log from the in situ measurements, all resistivity data that may have been affected by free water in hydraulically conductive fractures, detected in the in situ Posiva flow logging and inferred to as a flow anomalies, have to be sorted out. By examining the resistivity logs obtained by the Century 9072 tool, it has been found that resistivity values obtained within 0.5 m from a hydraulically conductive fracture (so called PFL anomaly) generally should be discarded. This distance includes a safety margin of 0.1–0.2 m.

4.2 Rock resistivity measurements in situ

4.2.1 Rock resistivity log KFR105

The rock resistivity of KFR105 was logged in June 2009 (Nielsen and Ringgaard 2009a). The in situ rock resistivity was obtained using the focused rock resistivity tool Century 9072. In situ rock resistivities, used in this present report, were obtained between the borehole lengths 4.04–305.14 m. In order to obtain an exact depth calibration, the track marks made in the borehole were used. According to Nielsen and Ringgaard (2009a, Section 5.2.4) an accurate depth calibration was obtained by somewhat stretching the scale of the logs. Numerical resistivity data used as input data to this present report have been taken from the SICADA database[1].

Figure 4-1 shows the distribution of the rock resistivities obtained in KFR105. The histogram ranges from 0–70,000 ohm.m and is divided into sections of 2,500 ohm.m. The arithmetic mean of all data points is 8,308 ohm.m.

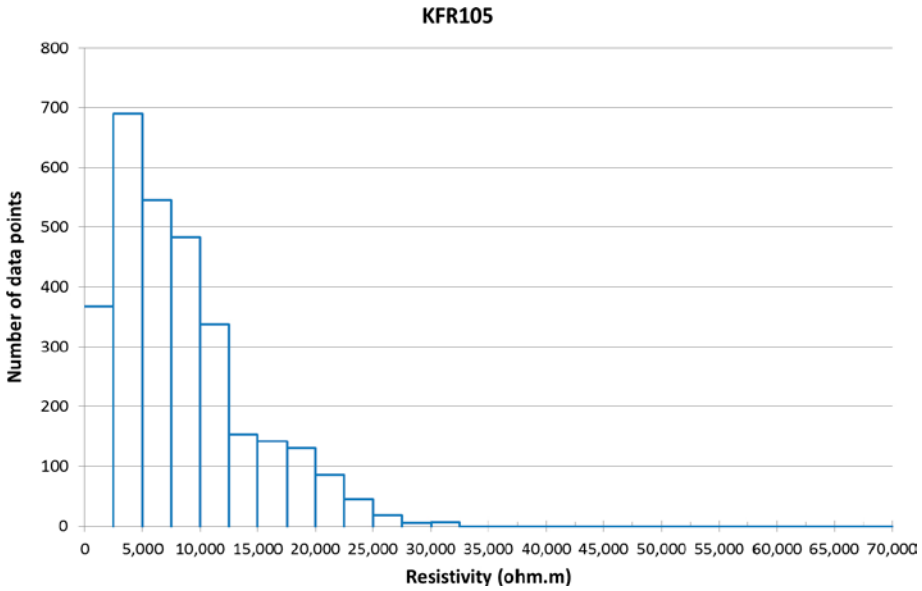

Figure 4-1. *Distribution of rock resistivities in KFR105.*

[1] DATA DELIVERY Sicada_12_091: GP162 – Focused resistivity 300 cm/ "focused resistivty.xls".

4.2.2 Rock matrix resistivity KFR105

All resistivity data obtained within a distance of less than 0.5 m from an open fracture, as interpreted in the borecore mapping, were sorted out from the in situ rock resistivity log. In the core log, a total of 1101 interpreted open fractures are recorded between the borehole lengths 0–306.8 m (cf. Winell 2009, Appendix 1). Nine zones where the core has been crushed or lost were recorded. A total of 0.56 m of the core is crushed or lost. Open fractures can potentially intersect the borehole in zones where the core is crushed or lost. Therefore, these zones were treated as continually containing open fractures when discarding rock resistivity data from the rock matrix resistivity log. The locations of open fractures in KFR105 are shown in Appendix A1. Numerical boremap data used as input data to this present report have been taken from the SICADA database[2]. By comparing dips in the resistivity log with locations of interpreted open fractures in the boremap log, it can be concluded that the recorded borehole lengths of the two logs are within ±0.1 m, which is judged to be acceptable.

A total of 264 rock matrix resistivities were obtained between 4.04–305.14 m. All of the rock matrix resistivities were within the stated quantitative measuring range of the Century 9072 tool. The rock matrix resistivity log is shown in Appendix A1. Numerical data are tabulated in Appendix B1.

Figure 4-2 shows the distribution of the rock matrix resistivities obtained in KFR105. The histogram ranges from 0–70,000 ohm.m and is divided into sections of 2,500 ohm.m. The arithmetic mean of all data points is 13,086 ohm.m.

4.2.3 Fractured rock resistivity KFR105

All resistivity data obtained within less than 0.5 m from a hydraulically conductive fracture, detected and interpreted in the difference flow logging (Väisäsvaara 2009, Appendix KFR105.7.1), were sorted out from the in situ rock resistivity log. A total of 150 hydraulically conductive fractures were detected in KFR105 between approximately 3–305 m. The locations of hydraulically conductive fractures are shown in Appendix A1. A total of 1,673 fractured rock resistivities were obtained between 4.04–305.14 m (it was implicitly assumed that there is no undetected flow anomaly in the last one metre of the borehole). All of the fractured rock resistivities were within the quantitative measuring range of the Century 9072 tool. The fractured rock resistivity log is shown in Appendix A1.

Figure 4-3 shows a histogram of the fractured rock resistivities obtained in KFR105. The histogram ranges from 0–70,000 ohm.m and is divided into sections of 2,500 ohm.m. The arithmetic mean of all data points is 9,168 ohm.m.

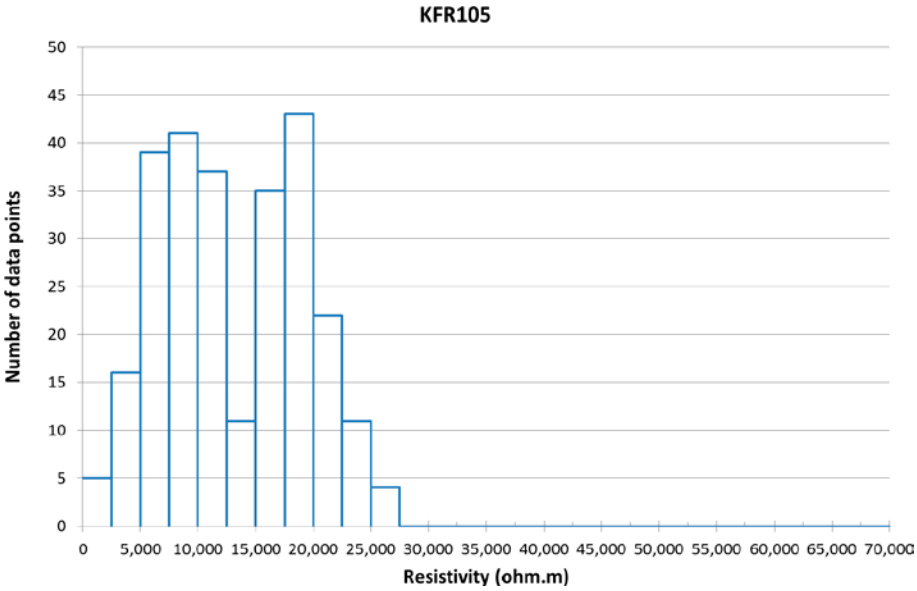

Figure 4-2. *Distribution of rock matrix resistivities in KFR105.*

[2] DATA DELIVERY Sicada_12_091: Boremap – “p_fract_core.xls”; “p_fract_crush.xls”; “p_core_loss.xls”.

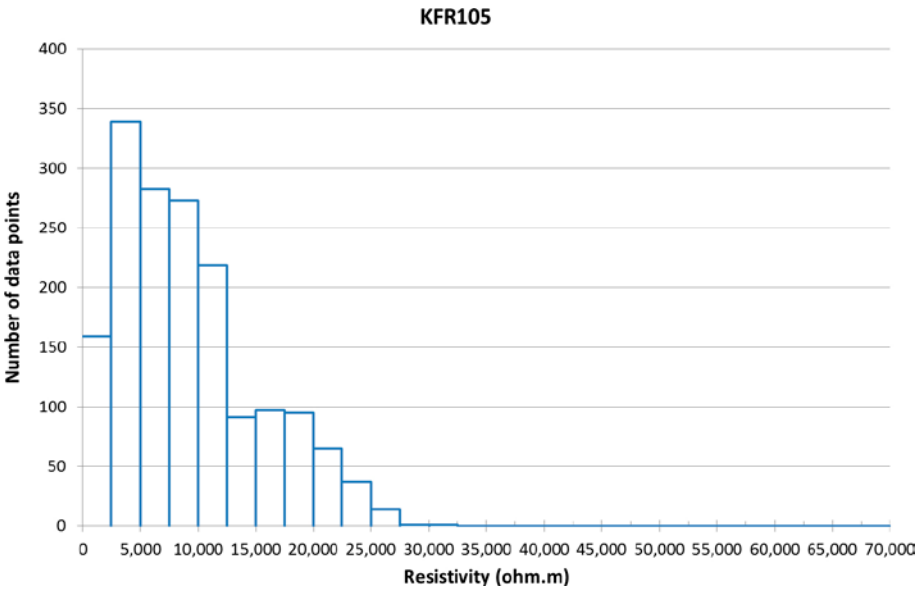

***Figure 4-3**. Histogram of fractured rock resistivities in KFR105.*

4.2.4 Rock resistivity KFR102B

The rock resistivity of KFR102B was logged in October 2008 (Nielsen and Ringgaard 2009b). The in situ rock resistivity was obtained using the focused rock resistivity tool Century 9072. In situ rock resistivities, used in this present report, were obtained between the borehole lengths 15.5–178.3 m. In order to obtain an exact depth calibration, the track marks made in the borehole were used. According to Nielsen and Ringgaard (2009b, Section 5.2.4) an accurate depth calibration was obtained by somewhat stretching the scale of the logs. Numerical resistivity data used as input data to this present report have been taken from the SICADA database[3].

Figure 4-4 shows the distribution of the rock resistivities obtained in KFR102B. The histogram ranges from 0–70,000 ohm.m and is divided into sections of 2,500 ohm.m. The arithmetic mean of all data points is 15,811 ohm.m.

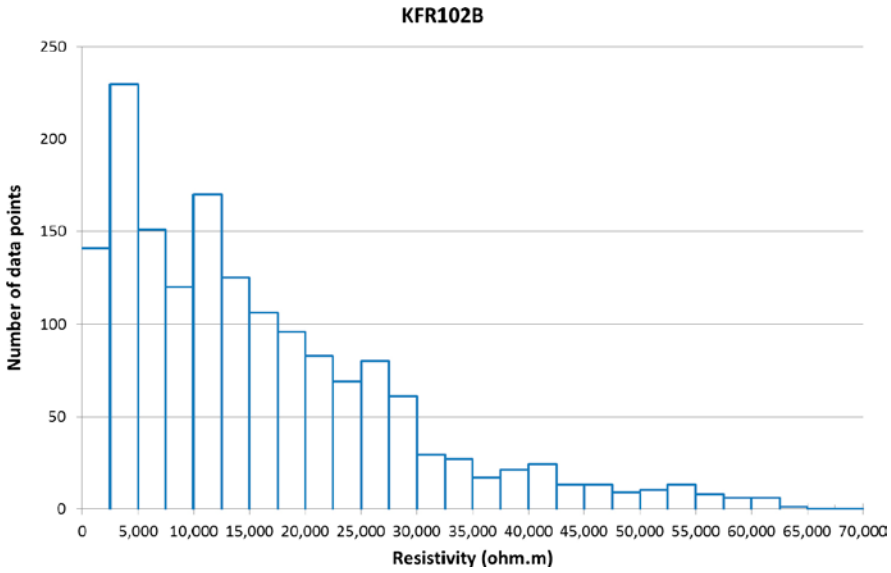

***Figure 4-4.** Distribution of rock resistivities in KFR102B.*

[3] DATA DELIVERY Sicada_12_091: GP162 – Focused resistivity 300 cm/ “focused resistivty.xls”.

4.2.5 Rock matrix resistivity KFR102B

All resistivity data obtained within less than 0.5 m from an open fracture, as interpreted in the borecore mapping, were sorted out from the in situ rock resistivity log. In the core log, a total of 618 interpreted open fractures are recorded between the borehole lengths 13.9–180.1 m (cf. Döse et al. 2009, Appendix 1). Three zones where the core has been crushed or lost were recorded. A total of 0.097 m of the core is crushed or lost. Open fractures can potentially intersect the borehole in zones where the core is crushed or lost. Therefore, these zones were treated as continually containing open fractures when discarding rock resistivity data from the rock matrix resistivity log. The locations of open fractures in KFR105 are shown in Appendix A1. Numerical boremap data used as input data to this present report have been taken from the SICADA database[4]. By comparing dips in the resistivity log with locations of interpreted open fractures in the boremap log, it can be concluded that the recorded borehole lengths of the two logs are within ±0.1 m, which is judged to be acceptable.

A total of 86 rock matrix resistivities were obtained between 15.5–178.3 m. 85% of the rock matrix resistivities were within the stated quantitative measuring range of the Century 9072 tool. The rock matrix resistivity log is shown in Appendix A2. Numerical data are tabulated in Appendix B2.

Figure 4-5 shows the distribution of the rock matrix resistivities obtained in KFR102B. The histogram ranges from 0–70,000 Ωm and is divided into sections of 2,500 ohm.m. The arithmetic mean of all data points is 29,321 ohm.m.

4.2.6 Fractured rock resistivity KFR102B

All resistivity data obtained within less than 0.5 m from a hydraulically conductive fracture, detected and interpreted in the difference flow logging (Kristiansson and Väisäsvaara 2008, Appendix KFR102B.7), were sorted out from the in situ rock resistivity log. A total of 89 hydraulically conductive fractures were detected in KFR102B between approximately14–174 m. The locations of hydraulically conductive fractures are shown in Appendix A1. A total of 901 fractured rock resistivities were obtained between 15.5–174 m. 96% of the fractured rock resistivities were within the stated quantitative measuring range of the Century 9072 tool. The fractured rock resistivity log is shown in Appendix A2.

Figure 4-6 shows a histogram of the fractured rock resistivities obtained in KFR102B. The histogram ranges from 0–70,000 ohm.m and is divided into sections of 2,500 ohm.m. The arithmetic mean of all data points is 19,338 ohm.m.

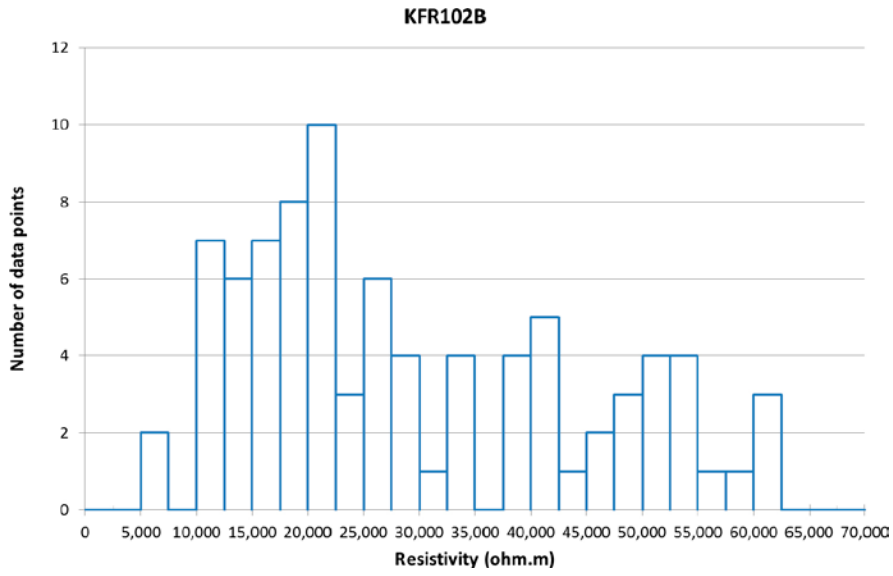

Figure 4-5. *Distribution of rock matrix resistivities in KFR102B.*

[4] DATA DELIVERY Sicada_12_091: Boremap – “p_fract_core.xls”; “p_fract_crush.xls”; “p_core_loss.xls”.

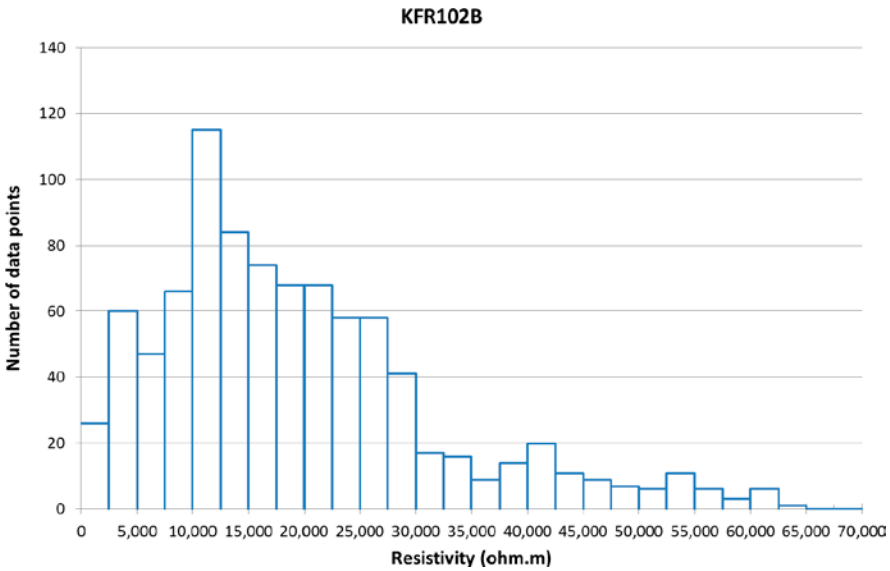

Figure 4-6. *Histogram of fractured rock resistivities in KFR102B.*

4.3 Groundwater EC measurements in situ

4.3.1 General comments

Data from two site investigation methods of obtaining the electrical conductivity (EC) of the groundwater have been used as input to this report. These methods are 1) fracture-specific EC from the Posiva flow log in boreholes KFR102B (Kristiansson and Väisäsvaara 2008) and KFR105 (Väisäsvaara 2009), and 2) hydrochemical characterisation of groundwater in five sections in KFR105 (Lindquist and Nilsson 2010).

No leaching of pore water fluid and subsequent chemical characterisation has been performed on drill core samples at the SFR site. Accordingly one is forced to assume that the pore water is reasonably well equilibrated with the groundwater, as has previously been shown to be a justified assumption at Forsmark at larger depths in e.g. Löfgren (2007). It should be noted that in order to be a major contributor to data uncertainty, there needs to be a substantial disequilibration between groundwater and rock matrix pore water. Such a substantial disequilibrium is more likely in shallow rock where the flow rates are higher than at deeply lying rock. Also, the presence of the SFR repository may have caused a disturbance in the groundwater situation, manifesting in groundwater compositions that deviate from the natural case. Based on long-term trend data from the hydrochemical monitoring programme, spanning from the 1980's up until recent times, such disturbance appears to be reasonably limited when it comes to the groundwater main constituents such as chloride (Nilsson A-C 2009, Appendix 3).

In the background reports concerning the EC of the groundwater (Kristiansson and Väisäsvaara 2008, Väisäsvaara 2009, Lindquist and Nilsson 2010), electrical conductivities have been corrected for temperature, so that they correspond to data at 25°C. Data that correspond to the temperature in situ should be used in in situ evaluations. For data from the Posiva flow log, electrical conductivities at in situ temperatures have been obtained from raw data files stored at the SICADA database. For data from the hydrochemical characterisation of groundwater, the temperature correction has been made according to Eq. 4-6 (Hayashi 2004).

$$EC_T = EC_{25}\big(1 - 0.019(T - 25)\big) \qquad \text{Equation 4-6}$$

Where EC_{25} (S/m) is the electrical conductivity at 25°C and T is the ambient temperature in °C. It should be noted that the temperature correction is slightly dependent on the groundwater composition and that slightly different relations are used in different applications. Also, the temperature of the extracted groundwater may not have to be the same as that of the rock matrix, in case of a large flow. This evokes minor data uncertainty that is dwarfed by seasonal and long-term variation of the rock temperature.

4.3.2 EC measurements in KFR105

The fracture-specific EC was measured at eight locations in borehole KFR105 (see Table 4-1) by using the Posiva flow log. The obtained data are shown in Figure 4-7 as black crosses, indicating the last measured data point of the transient (time series) fracture-specific EC measurement. The purple dots represent transient fracture-specific ECs. The EC of the borehole fluid was measured before and after performing flow measurements and fracture-specific EC measurements, i.e. before and after performing extensive pumping (Väisäsvaara 2009). The curves in Figure 4-7 represent the borehole fluid EC logs obtained before (light green) and after (dark green) the pumping.

As can be in Figure 4-7, the borehole fluid EC obtained prior to, and after, the pumping does not deviate much from the fracture-specific EC. This is expected as the borehole is drilled from a tunnel. Accordingly there is a natural inflow from the surrounding rock into the borehole even when no pumping is performed (cf. Väisäsvaara 2009, Appendix KFR105.6.1). Numerical data on the obtained fracture-specific electrical conductivities are shown in Table 4-1.

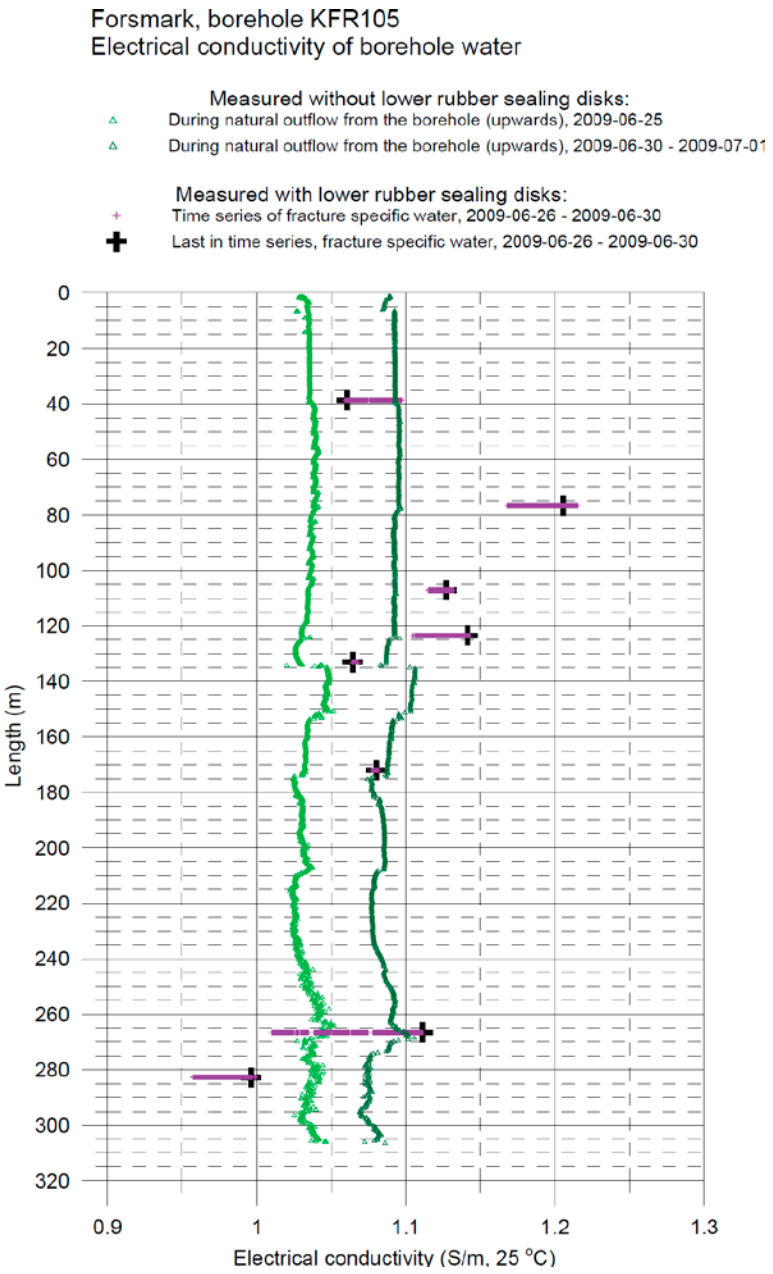

Figure 4-7*. EC logs in KFR105. Image reproduced from Väisäsvaara (2009, Appendix KFR105.2.1).*

The groundwater EC of has also been measured in hydrochemical characterisations of groundwater in five sections in KFR105 (Lindquist and Nilsson 2010). In these five sections, groundwater has been withdrawn from the borehole on numerous occasions and measured in the laboratory. In addition, in two of the sections an online in situ electrical conductivity electrode has continuously recorded data. Table 4-2 shows the mean value of the laboratory measurements for each section, as well as the representative EC from the online measurements. The data are both given at 25°C, as displayed in Lindquist and Nilsson (2010), and at the in situ temperature. To obtain the latter data, a temperature correction was made by using Eq. 4-6. For the online measurements in sections 120–173 m and 256.0–306.8 m, the representative in situ temperature 11.5 and 11.3°C were given (Lindquist and Nilsson 2010, Table A3-1). Based on this, it is assumed that the entire borehole had the constant temperature of 11.4°C during the hydrochemical measurements.

As can be seen from Table 4-1 and Table 4-2, the spread in data at the in situ temperature is small and there is no significant trend (at least not if comparing to the overall data uncertainty involved in obtaining in situ formation factors). This is illustrated in Figure 4-8 for the EC at 25°C. The bars represent the individual laboratory measurements from the hydrochemical characterisation. The diamonds represents the fracture-specific water from the Posiva flow log.

Based on the above, it has been decided to assume a constant EC of 0.73 S/m in the entire borehole. This value corresponds to the data from the two online measurements, which likely are the most accurate measurements of the ones presented. Also, this value corresponds to the arithmetic mean of all the EC values at in situ temperature displayed in Table 4-1 and Table 4-2.

Table 4-1. Fracture-specific ECs from Posiva flow log, KFR105.

Section[a] Borehole section (m)	Location of fracture[a] Borehole length (m)	EC 25°C[a] (S/m)	EC at in situ temperature[b] (S/m)
38.65–39.65	39.4	1.06	0.70
76.64–77.64	77.3	1.21	0.79
107.20–108.20	107.7	1.13	0.74
123.49–124.49	124.1	1.14	0.75
133.10–134.10	133.7	1.07	0.70
172.06–173.06	172.7, 173.0	1.08	0.71
266.51–267.51	267.3	1.11	0.73
282.79–283.79	283.5	1.00	0.65

[a] Data from Väisäsvaara (2009, Table 6-2).

[b] Data from SICADA, DATA DELIVERY Sicada_12_091: HY684, plu_pfl_fracture_ec.xls (last data in each time series). The in situ temperature was around 7°C (Väisäsvaara 2009, Appendix KFR105.2.3).

Table 4-2. Groundwater ECs in different sections from hydrochemical characterisation, KFR105.

Borehole section (m)	Laboratory or online measurement	EC at 25°C (S/m)	EC at in situ temperature[c] (S/m)
4.0–119.0	Lab	1.09 [a]	0.80
120.0–137.0	Lab	1.01 [a]	0.75
120.0–137.0	Online	0.98 [b]	0.73
138.0–169.0	Lab	1.08 [a]	0.80
170.0–264.0	Lab	1.00 [a]	0.74
256.0–306.8	Lab	0.99 [a]	0.73
256.0–306.8	Online	0.99 [b]	0.73

[a] Mean value of four to six separate laboratory EC measurements, documented in Lindquist and Nilsson (2010, Table A3-1).

[b] EC from the online measurements taken from Lindquist and Nilsson (2010, Table 7-1).

[c] EC at in situ temperature 11.4°C, corrected by Eq. 4-6.

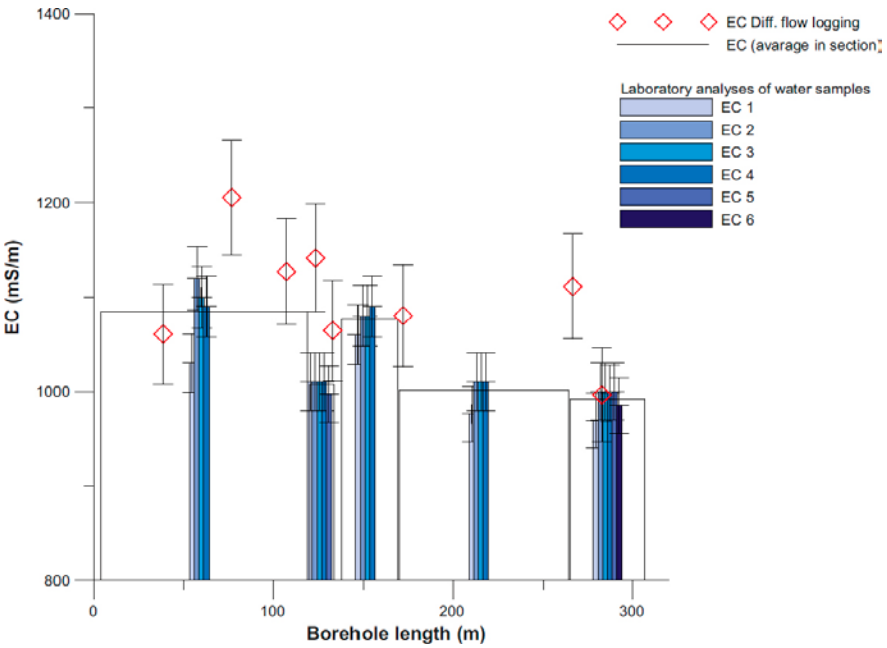

Figure 4-8. *EC at 25°C in KFR105 from hydrochemical characterisation and Posiva flow log. Figure reproduced from Lindquist and Nilsson (2010, Figure 5-2).*

4.3.3 EC measurements in KFR102B

The fracture-specific EC was measured at five locations in borehole KFR102B (see Table 4-3) by using the Posiva flow log (Kristiansson and Väisäsvaara 2008). The obtained data are shown in Figure 4-9 as black crosses, indicating the last measured data point of the transient (time series) fracture-specific EC measurement. The purple dots represent transient fracture-specific ECs. The EC of the borehole fluid was measured before and during pumping. The lines in Figure 4-9 represent the borehole fluid EC logs obtained before (blue) and during (green) the pumping.

As can be seen in Figure 4-9, the borehole fluid EC obtained prior to and during the pumping somewhat deviate from the fracture-specific EC. It appears that more saline water has penetrated down the borehole prior to the measurements, and that the water flowing from the fractures into the borehole while pumping is less saline. Judging solely from the transient part of the fracture-specific EC measurements (Kristiansson and Väisäsvaara 2008, Appendix KFR102B.11), the values at the borehole lengths 126.9 and 171.4 m appears to be the most reliable[5]. However, as fracture water naturally flows into the borehole in the upper 90 or so metres (Kristiansson and Väisäsvaara 2008, Appendix KFR102B.6.1) also the shallow values should be reasonably accurate. Numerical data on the obtained fracture-specific electrical conductivities are shown in Table 4-3.

Based on the data in Table 4-3, one may assume a constant EC of 0.60 S/m in the entire borehole. However, this assumption may not be valid for the uppermost part of the borehole, where the rock mass may be affected by infiltrating meteoric water. However, this is not an limitation for this present report, as no in situ formation factors can be assessed in the upper 15 m of the borehole due to lack of rock resistivity data. This facilitates a decision where the constant EC of 0.60 S/m is assumed below the borehole length 15 m. This assumption would mean a chloride concentration of about 3,000 mg/L (cf. Nilsson et al. 2010, Figure 4-4) along the borehole. This is in line with the measured chloride concentrations in other boreholes at the site, for the upper 150 m (Nilsson et al. 2010, Figure 6-2a). It is also in line with the chloride concentration of the local Baltic Sea[6].

[5] They seem reliable as the EC clearly deviates from that of the drillhole fluid, as the curves level out at the final part of the time series, and as there is little scatter.

[6] One of the groundwater types used in site descriptive modelling (cf. Nilsson et al. 2010, Section 3.3).

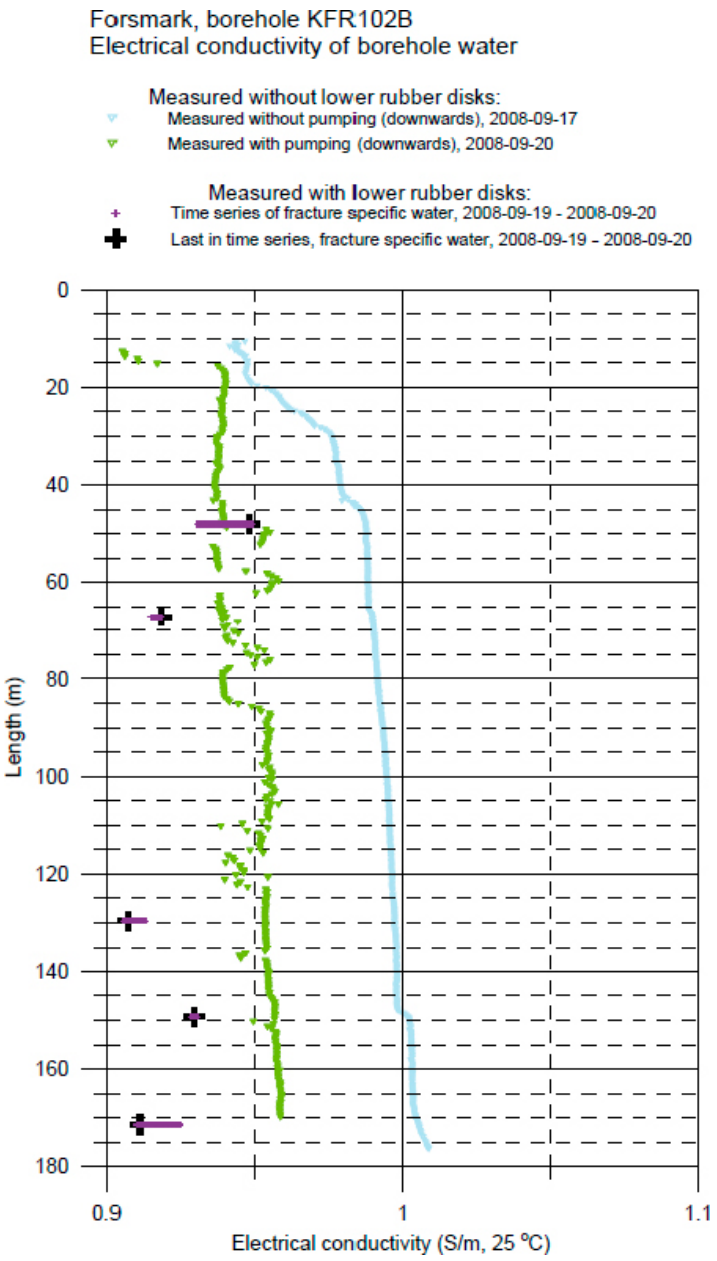

Figure 4-9. *EC logs in KFR102B. Image reproduced from Kristiansson and Väisäsvaara (2008, Appendix KFR102B.2.2).*

Table 4-3. Fracture-specific ECs from Posiva flow log, KFR102B.

Borehole section (m)	Location of fracture[a] Borehole length (m)	EC 25°C[a] (S/m)	EC at in situ temperature[b] (S/m)
48.01–49.01	48.2, 48.7	0.95	0.62
67.03–68.03	67.7	0.92	0.59
129.63–130.63	130.3	0.91	0.59
149.25–150.25	149.8	0.93	0.60
171.38–172.38	172.0	1.91	0.59

[a] Data from Kristiansson and Väisäsvaara (2008, Table 6-3).

[b] Data from SICADA, DATA DELIVERY Sicada_12_091: HY684, plu_pfl_fracture_ec.xls (last data in each time series). The in situ temperature was around 7°C below borehole length 20 m (Kristiansson and Väisäsvaara 2008, Appendix KFR102B.2.3).

4.3.4 Electrical conductivity of the pore water

As there are no direct measurements on rock matrix pore water, the assumption has to be made that the groundwater is well equilibrated with the pore water. This results in the following assumptions concerning the electrical conductivity of the pore water in the rock mass surrounding the two boreholes.

KFR105: borehole length 0–306 m,

$$EC\ (S/m) = 0.73\ S/m \qquad \text{Equation 4-7}$$

KFR102B: borehole length 15–180 m,

$$EC\ (S/m) = 0.60\ S/m \qquad \text{Equation 4-8}$$

Based on experience from the site investigation for the KBS-3 repository at Forsmark, it is judged as likely that the pore water EC should not be less than 50% or more than 200% of the assumed values. Also, it is judged that the assumption is better for relatively deeply situated rock than for shallow rock.

5 Results

As described above, from the rock resistivity and electrical conductivity of the pore water, the apparent formation factor can be obtained (Eq. 4-4). These apparent formation factors can be corrected into formation factors (Eq. 4-5). The in situ formation factors obtained in KFR105 and KFR102B have been treated statistically. In doing this, the mean value and standard deviation[7] of $\log_{10}(F_f)$ have been calculated and the corresponding log-normal distribution is plotted. This is compared to a histogram of the corresponding data. Also cumulative distribution functions of the data are plotted.

5.1 In situ rock matrix formation factor

In borehole KFR105 a total of 264 rock matrix formation factors, F_f^{rm}, were obtained in situ between the borehole lengths 4.04–305.14 m. Figure 5-1 shows the histogram and fitted log-normal distribution of the obtained data. The arithmetic mean of the rock matrix formation factors is 1.1×10^{-4}. Distribution parameters, as well as the arithmetic mean, are tabulated in Table 5-1. The in situ rock matrix formation factor log of KFR105 is shown in Appendix C1. A histogram of the rock matrix apparent formation factor is shown in Appendix D1.

In borehole KFR102B a total of 86 rock matrix formation factors were obtained in situ between the borehole lengths 15.5–178.3 m. Figure 5-2 shows the histogram and fitted log-normal distribution of the obtained data. The arithmetic mean of the rock matrix formation factors is 4.7×10^{-5}. Distribution parameters, as well as the arithmetic mean, are tabulated in Table 5-1.The in situ rock matrix formation factor log of KFR102B is shown in Appendix C2. A histogram of the rock matrix apparent formation factor is shown in Appendix D2.

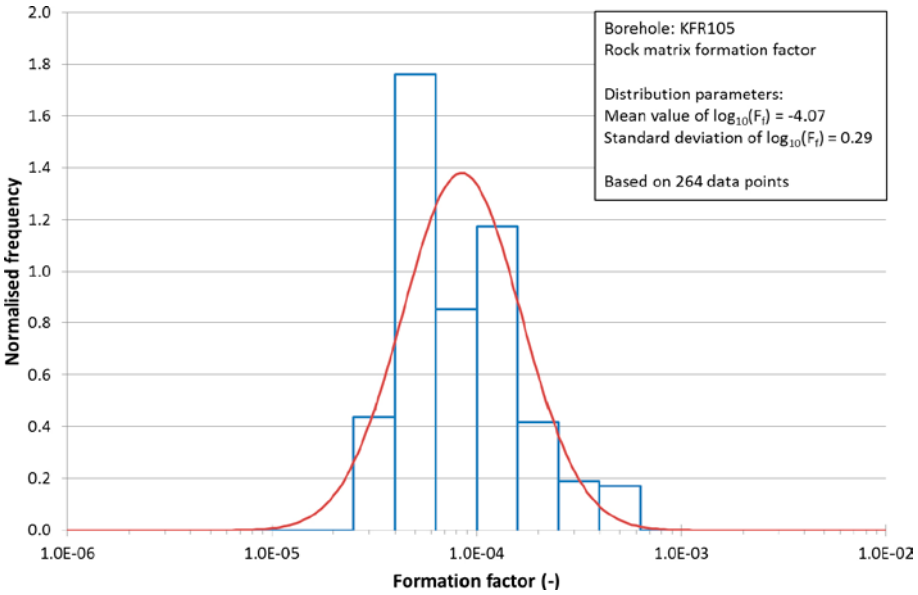

Figure 5-1. *Rock matrix formation factors of borehole KFR105.*

[7] It should be noted that in this present report, as opposed to in previous corresponding site investigation reports, apparent formation factors have already been corrected into formation factors. Therefore there should be no "lower measurement limit" of the formation factors (originating in artifacts due to surface conduction). Accordingly, the mean value and standard deviation can be obtained in a traditional way (in this exercise using the commands AVERAGE and STDEV in MS Excel), as opposed to the normal-score method as used previously (e.g. Löfgren and Neretnieks 2005a, Section 5.3).

Table 5-1. Distribution parameters and arithmetic mean value of the formation factor, KFR105 and KFR102B.

In situ formation factor	Number of data points	Mean $\log_{10}(F_f)$	Standard deviation $\log_{10}(F_f)$	Arithmetic mean F_f (–)
KFR105 Rock matrix F_f	264	–4.07	0.29	1.1×10^{-4}
KFR105 Fractured rock F_f	1,673	–3.84	0.38	2.2×10^{-4}
KFR102B Rock matrix F_f	86	–4.45	0.33	4.7×10^{-5}
KFR102B Fractured rock F_f	901	–4.17	0.40	1.1×10^{-4}

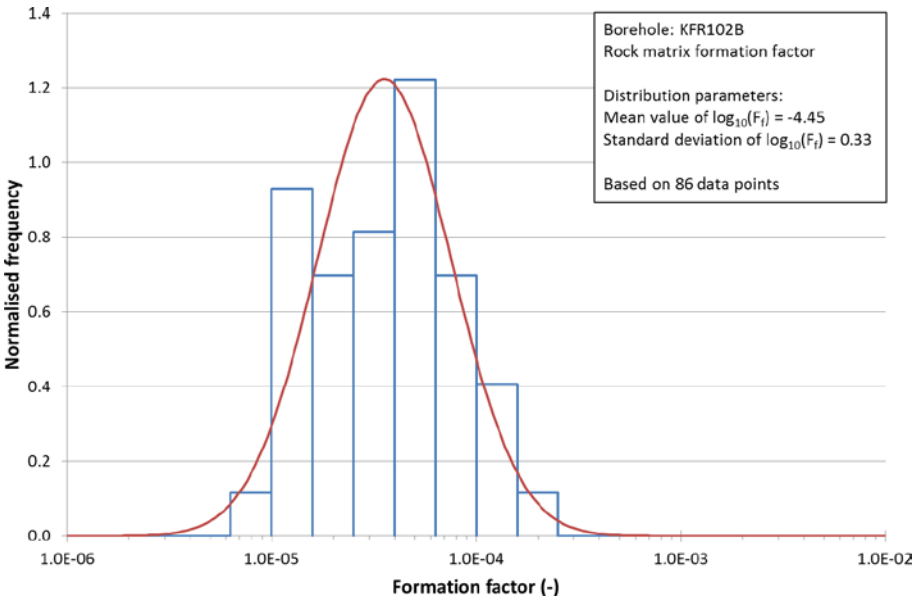

Figure 5-2. *Rock matrix formation factors of borehole KFR102B.*

5.2 In situ fractured rock formation factor

In borehole KFR105 a total of 1,673 fractured rock formation factors, F_f^{fr}, were obtained in situ between the borehole lengths 4.04–305.14 m. Figure 5-3 shows the histogram and fitted log-normal distribution of the obtained data. The arithmetic mean of the fractured rock formation factors is 2.2×10^{-4}. Distribution parameters, as well as the arithmetic mean, are tabulated in Table 5-1. The in situ fractured rock formation factor log of KFR105 is shown in Appendix C1.

In borehole KFR102B a total of 901 fractured rock formation factors were obtained in situ between the borehole lengths 15.5–174.0 m. Figure 5-4 shows the histogram and fitted log-normal distribution of the obtained data. The arithmetic mean of the fracture rock formation factors is 1.1×10^{-4}. Distribution parameters, as well as the arithmetic mean, are tabulated in Table 5-1. The in situ fractured rock formation factor log of KFR102B is shown in Appendix C2.

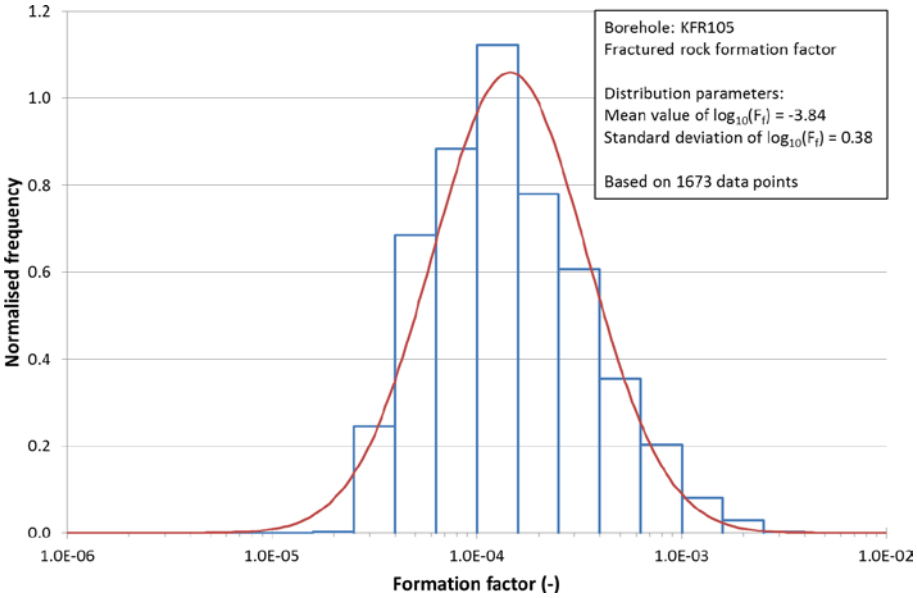

Figure 5-3. *Fractured rock formation factors of borehole KFR105.*

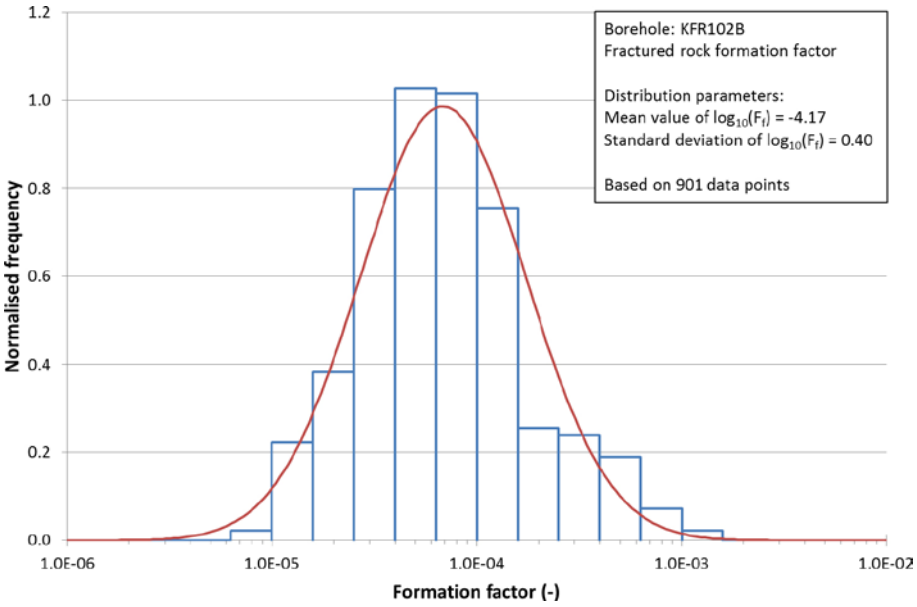

Figure 5-4. *Fractured rock formation factors of borehole KFR102B.*

5.3 Comparison of formation factors

Table 5-1 presents mean values and standard deviations of the log-normal distributions shown in Sections 5.1 and 5.2 for KFR105 and KFR102B. In addition, the number of data points obtained and the arithmetic mean values for the different formation factors are shown.

Figure 5-5 shows the cumulative distribution functions (CDFs) of the two different formation factors of KFR105 and KFR102B. As a comparison the corresponding CDF for the in situ rock matrix formation factor for the rock volume planned to host the KBS-3 repository at Forsmark is shown (SKB 2010a, Figure 6-80).

As can be seen for the rock matrix formation factor, the values at the SFR site are generally higher than for the KBS-3 host rock. For comparison, the arithmetic mean of the rock matrix formation factor for the KBS-3 host rock, as derived for the safety assessment SR-Site, is 2.11×10^{-5}. An explanation for this may be that the stress situation is different at the SFR site, which is outside the tectonic lens, compared to inside the tectonic lens. In addition, the data from site investigation SFR are obtained at shallower depths compared to those obtained within site investigation Forsmark. Accordingly, they are subjected to less stress from the overburden. The deviations may also be explained by differences in rock type and lithology.

For boreholes KFR105 and KFR102B the fractured rock formation factors are generally higher that the rock matrix formation factors, as expected. Generally, the formation factors of borehole KFR105 are higher than those of KFR102B. Four possible explanations to this are given below:

1. The boreholes are surrounded by different rock types having different lithology; manifesting in different geometric properties of the microporous network. For example, the highest rock resistivities in KFR102B seem to correspond to the rock type amphibolite (Döse et al. 2009, Appendix 1). This rock type is much less abundant in borehole KFR105 (Winell 2009, Appendix 1).
2. The pore waters of the different rock volumes surrounding the boreholes may differ more than the assumed values 0.60 S/m for KFR102B and 0.73 S/m for KFR105. If the rock volumes are similar with respect to the formation factor, this would indicate less saline water surrounding KFR102B than assumed, alternatively a more saline water surrounding KFR105 than assumed (or a combination of both). A way of testing this is to examine the formation factor of borehole sections surrounded by similar rock types. In doing this, the sections 89–130 m in KFR105 and 48–82 m in KFR102B were selected. According to Döse et al. (2009, Appendix 1) and Winell (2009, Appendix 1) both these sections mainly consist of the rock type "granite to granodiorite, metamorphic, medium-grained" with the rock type code 101057. In these sections, the arithmetic mean of the rock matrix formation factor is 1.1×10^{-4} for KFR105 and 7.7×10^{-5} for KFR102B. These two numbers are too similar to indicate a significant error in the assumption of relative pore water ECs. On the other hand, the notion of important differences in pore water EC of the rock volumes cannot be discarded solely based on this examination.
3. The boreholes are drilled in different directions. KFR105 is drilled from a tunnel, allowing for an almost horizontal borehole. Therefore, in case the rock matrix features anisotropy this may explain the differences in the data between the boreholes.
4. The borehole KFR102B is on average shallower than KFR105. Both boreholes at the SFR site are on average shallower than the investigated rock volumes for the KBS-3 repository. The closer to the ground surface the investigated rock is, the less is the weight of the overburden and the less the microporous system is compressed. Also, heavily fractured rock may be more stress released than sparsely fractured rock. The investigated rock volume at the SFR site has a higher degree of fracturing than the intended KBS-3 host rock. For KFR105, the part closest to the tunnel may have been subjected to stress-release as result of the excavation. However, such a potential effect should only be visible in the first few tenths of meters of the borehole.

Numerical values corresponding to the CDFs in Figure 5-5 are provided in Table 5-2.

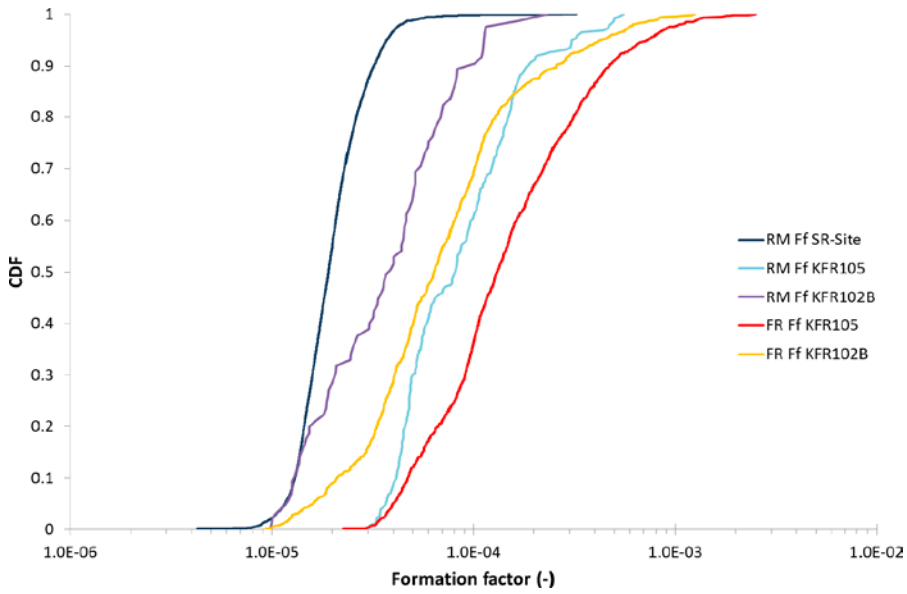

Figure 5-5. *CDFs for the rock matrix formation factor (labelled RM Ff) and fractured rock formation factor (labelled FR Ff) in boreholes KFR105, KFR102B and the host rock for the planned KBS-3 in Forsmark used in the safety assessment SR-Site.*

Table 5-2. Numerical values for use when recreating the CDFs of Figure 5-5. Values are intentionally provided in MS Excel format.

CDF%	F_f^{rm} (–) KFR105	F_f^{fr} (–) KFR105	F_f^{rm} (–) KFR102B	F_f^{fr} (–) KFR102B
0	2.9E–05	2.3E–05	9.8E–06	9.4E–06
1	3.2E–05	3.3E–05	9.9E–06	1.1E–05
3	3.4E–05	3.7E–05	1.1E–05	1.3E–05
5	3.7E–05	4.0E–05	1.2E–05	1.6E–05
10	4.2E–05	4.7E–05	1.3E–05	2.1E–05
20	4.6E–05	6.7E–05	1.5E–05	3.3E–05
30	5.0E–05	9.1E–05	2.1E–05	4.1E–05
40	5.9E–05	1.1E–04	3.1E–05	5.0E–05
50	8.1E–05	1.3E–04	3.9E–05	6.4E–05
60	9.7E–05	1.6E–04	4.6E–05	8.1E–05
70	1.2E–04	2.2E–04	5.5E–05	1.0E–04
80	1.5E–04	3.1E–04	6.9E–05	1.3E–04
90	1.9E–04	4.7E–04	1.0E–04	2.6E–04
95	3.1E–04	7.3E–04	1.1E–04	4.3E–04
97	4.4E–04	8.8E–04	1.2E–04	5.7E–04
99	5.0E–04	1.3E–03	1.7E–04	8.2E–04
100	2.5E–03	2.5E–03	2.3E–04	1.3E–03

6 Recommended effective diffusivities for use in SR-PSU

In this chapter, rock matrix effective diffusivities of the SFR host rock are recommended for use in the safety assessment SR-PSU. When using effective diffusivities to estimate the diffusive exchange between flowpaths and the rock matrix in safety assessment modelling, data should be flowpath averaged. The flowpath averaging means, in simplistic terms, that the contributions to retention in all small scale rock volumes along the flowpath are given the same weight when summarising the total retention[8]. If the flowpath is surrounded by rock volumes of near constant diffusive properties, or the diffusive properties are randomised on a scale that is small compared to the flowpath length, the spatial variability of the formation factor is of no concern. Accordingly a single point value of the formation factor can be used. If the flowpath intersects rather large rock volumes having different diffusive properties, different formation factors may have to be assigned for each rock volume. The data from the two investigated boreholes KFR105 and KFR102B, as well as data from the Oskarshamn site investigation (cf. SKB 2010b, Figure A8-4) and Forsmark site investigation (cf. SKB 2010a, Figure 6–77) suggest that in the investigated types of host rock, different rock volumes do not display major differences in formation factor distributions. In this context a major difference would mean an order of magnitude difference or more in the average formation factor. Based on this knowledge, it should be sufficient to assign a single point flowpath averaged formation factor for the entire SFR site for large-scale solute transport calculations. The use of a single point flowpath averaged formation factor for all flowpaths also requests that there is no major anisotropy effect. The absence of such major anisotropy effect is supported by the relatively small difference in the arithmetic mean of formation factors from KFR105 and KFR102B, where one of the boreholes is almost horizontal and the other is almost vertical.

When assigning a flowpath averaged formation factor to the SFR host rock, each data point obtained in this study is assigned equal importance. This means that all obtained data are pooled when calculating their arithmetic mean. In this respect, the probabilistic distributions associated with each borehole are not directly used for calculating the flowpath averaged formation factor. Instead, they are used for comparisons and their similarities lend weight to the general notion that different rock volumes at the site display similar behaviour when it comes to the formation factor. It should be noted that if performing small-scale and local modelling, for example if assessing a sharp redox front very close to ground surface, one may need to derive locally representative formation factors and effective diffusivities.

When assigning the effective diffusivity to be used in large-scale radionuclide transport modelling within SR-PSU, a starting point is the rock matrix formation factor. The choice of the rock matrix formation factor over the fractured rock formation factor is justified as it is generally more pessimistic, when assessing radionuclide release, to account for a smaller portion of the retention capacity of the bedrock. While the rock matrix formation factor corresponds to the retention capacity of the non-fractured rock matrix only, the fracture rock formation factor also accounts for the retention capacity in open fractures holding stagnant water.

As discussed above, it is assumed that each data point obtained in KFR105 and KFR102B is as representative as the other, in respect of having diffusive properties similar to those of the rock surrounding a typical flowpath between the SFR repository and ground surface. As the suggested diffusive properties should be flowpath averaged, the arithmetic mean of all the 350 rock matrix formation factors obtained is calculated, which results in $F_f^{rm} = 9.4\times10^{-5}$.

[8] If incorporating decay chains in the solute transport modelling, the situation may be somewhat more complicated.

By using Eq. 4-1 the formation factor can be converted to effective diffusivity. However, in doing this uncertainty is introduced as the diffusivity in free pore water, D_w, may vary for a radionuclide. Reasons for this may be variations in temperature, radionuclide speciation, or groundwater composition. Also, if the radionuclide is anionic there will be an anion exclusion effect. The consequences of this additional uncertainty are further discussed in the SR-Site data report (SKB 2010a, Section 6.8) which is referred to for background information. By using the SR-Site approach, the recommended effective diffusivity for use in SR-PSU radionuclide transport modelling is given in Table 6-1. In doing this, the best estimate D_w is assumed to be 1.0×10^{-9} m^2/s.

By inserting the flowpath averaged rock matrix formation factor and the best estimate D_w into Eq. 4-1; $\log_{10}(D_e) = -13.0$. In SR-Site it was argued that a reasonable way of accounting for data uncertainty is to use this value as mean, μ, in a log-normal distribution with a standard deviation, σ, of 0.25 log units. To account for anion exclusion, which lowers the effective diffusivity for anions compared to for neutral species, it was recommended to shift the entire probability density function downwards by 0.5 log units (cf. SKB 2010a, Table 6-91). By using these recommendations one ends up with the data set in Table 6-1. It should be noted that in the review of SR-Site conducted by the Swedish Radiation Safety Authority (SSM 2013, Haggerty 2012), this rather low standard deviation of 0.25 log units was questioned. In reports recently provided by SKB to SSM, this is discussed. The conclusions are that 1) using a standard deviation of only 0.25 log units is probably on the lower side, and 2) the effect of the uncertainty in this standard deviation is dwarfed by the effect of choosing the pessimistic approach of assuming that the flowpaths are bounded by undisturbed rock. Except for disregarding diffusion into stagnant water volumes in open fractures intersecting the flowpaths, additional retention in altered rock along the flowpaths is disregarded. Given the fact that the additional analyses provided by SKB have been conducted at a very late stage of the SR-PSU project, and that the general conclusion is that the approach taken in SR-Site is pessimistic, it has been decided not to change the recommendations to SR-PSU based on these new analyses.

For other solute transport applications than radionuclide retention modelling, the modeller may find it appropriate to use the fractured rock formation factor. The arithmetic mean of all the 2,574 fractured rock formation factors obtained in KFR105 and KFR102B equals 1.8×10^{-4}. It may be conceptually unclear to what extent the fractured rock formation factor represents the combined effect of diffusive exchange between flowpaths and the rock matrix and stagnant water in intersecting open fractures. However, in some solute transport applications it may not necessarily be conservative to use the lowest diffusive exchange rate, but instead pessimistic to use the higher value represented by the fractured rock formation factor.

Table 6-1. Flowpath averaged in situ effective diffusivity suggested for use in SR-PSU radionuclide transport modelling.

Type of solute	Best estimate *De* (m^2/s)	$\log_{10}(D_e)$ μ	$\log_{10}(D_e)$ σ	Probability density function
Cations and non-charged	9.4×10^{-14}	–13.0	0.25	Log-normal
Anions	3.2×10^{-14}	–13.5	0.25	Log-normal

References

SKB's (Svensk Kärnbränslehantering AB) publications can be found at www.skb.se/publications. References to SKB's unpublished documents are listed separately at the end of the reference list. Unpublished documents will be submitted upon request to document@skb.se.

Crawford J, 2008. Bedrock transport properties Forsmark. Site descriptive modelling SDM-Site Forsmark. SKB R-08-48, Svensk Kärnbränslehantering AB.

Döse C, Winell S, Stråhle A, Carlsten S, 2009. Site investigation SFR. Boremap mapping of core drilled boreholes KFR102B and KFR103. SKB P-09-38, Svensk Kärnbränslehantering AB.

Haggerty R, 2012. Review of matrix diffusion and related properties of intact rock in SKB's licence application for a spent nuclear fuel repository in Forsmark, Sweden. Technical note 2012:44, Strålsäkerhetsmyndigheten (Swedish Radiation Safety Authority).

Hayashi M, 2004. Temperature–electrical conductivity relation of water for environmental monitoring and geophysical data inversion. Environmental Monitoring and Assessment 96, 119–128.

Kristiansson S, Väisäsvaara J, 2008. Site investigation SFR. Difference flow logging in boreholes KFR102B and KFR103. SKB P-08-99, Svensk Kärnbränslehantering AB.

Lindquist A, Nilsson K, 2010. Site investigation SFR. Hydrochemical characterisation of groundwater in borehole KFR105. Results from five investigated borehole sections. SKB P-10-02, Svensk Kärnbränslehantering AB.

Löfgren M, 2007. Forsmark site investigation. Formation factor logging in situ by electrical methods in KFM01D and KFM08C. SKB P-07-138, Svensk Kärnbränslehantering AB.

Löfgren M, Neretnieks I, 2005a. Oskarshamn site investigation. Formation factor logging in situ and in the laboratory by electrical methods in KSH01A and KSH02. Measurements and evaluation of methodology. SKB P-05-27, Svensk Kärnbränslehantering AB.

Löfgren M, Neretnieks I, 2005b. Forsmark site investigation. Formation factor logging in situ by electrical methods in KFM01A and KFM02A. Measurements and evaluation of methodology. SKB P-05-29, Svensk Kärnbränslehantering AB.

Löfgren M, Vecernik P, Havlova V, 2009. Studying the influence of pore water electrical conductivity on the formation factor, as estimated based on electrical methods. SKB R-09-57, Svensk Kärnbränslehantering AB.

Nielsen U T, Ringgaard J, 2009a. Site investigation SFR. Geophysical borehole logging in boreholes KFR105 and HFM07. SKB P-09-76, Svensk Kärnbränslehantering AB.

Nielsen U T, Ringgaard J, 2009b. Site investigation SFR. Geophysical borehole logging in the boreholes KFR27 (0–500 m), KFR102A, KFR102B, KFR103, KFR104 and HFM07. SKB P-09-16, Svensk Kärnbränslehantering AB.

Nilsson A-C, 2009. Site investigation SFR. Presentation and evaluation of hydrogeochemical data from SFR-boreholes, 1984–2007. SKB P-09-45, Svensk Kärnbränslehantering AB.

Nilsson A-C, Tullborg E-L, Smellie J, 2010. Preliminary hydrogeochemical site description SFR (version 0.2). SKB R-10-38, Svensk Kärnbränslehantering AB.

Nilsson G, 2009. Site investigation SFR. Drilling of the cored borehole KFR105. SKB P-09-41, Svensk Kärnbränslehantering AB.

Nilsson G, Ullberg A, 2009. Drilling of the cored boreholes KFR101, KFR102B, KFR103 and KFR104. SKB P-09-13, Svensk Kärnbränslehantering AB.

SKB, 2010a. Data report for the safety assessment SR-Site. SKB TR-10-52, Svensk Kärnbränslehantering AB.

SKB, 2010b. Comparative analysis of safety related site characteristics. SKB TR-10-54, Svensk Kärnbränslehantering AB.

SSM, 2013. Begäran om komplettering av ansökan om slutförvaring av använt kärnbränsle och kärnavfall – Retardation av radionuklider. SSM2011-2426-110, Strålsäkerhetsmyndigheten (Swedish Radiation Safety Authority). (In Swedish.)

Thomson G, Miller A, Smith G, Jackson D, 2008. Radionuclide release calculations for SAR-08. SKB R-08-14, Svensk Kärnbränslehantering AB.

Vecernik P, Havlova V, Löfgren M, 2012. Determination of rock migration parameters (F_f, D_e): application of electromigration method on samples of different length. In Rabung T, Molinero J, Garcia D, Montoya V (eds). 1st Workshop proceedings of the collaborative project "Crystalline Rock Retention Processes" (7th EC FP CP CROCK). Karlsruhe: Karlsruhe Institute of Technology. (KIT Scientific Reports 7629), 137–147.

Väisäsvaara J, 2009. Site investigation SFR. Difference flow logging in borehole KFR105. SKB P-09-09, Svensk Kärnbränslehantering AB.

Winell S, 2009. Site investigation SFR. Boremap mapping of core drilled borehole KFR105. SKB P-09-59, Svensk Kärnbränslehantering AB.

Unpublished documents

SKBdoc id, version	Title	Issuer, year
1417017 ver 1.0	Artefacts associated with electrical measurements of the rock matrix formation factor – response to the request by SSM for supplementary information on retention of radionuclides (SSM2011-2426-110)	SKB, 2014

Appendix A

A1 In situ rock resistivities, open fractures, and flow anomalies KFR105

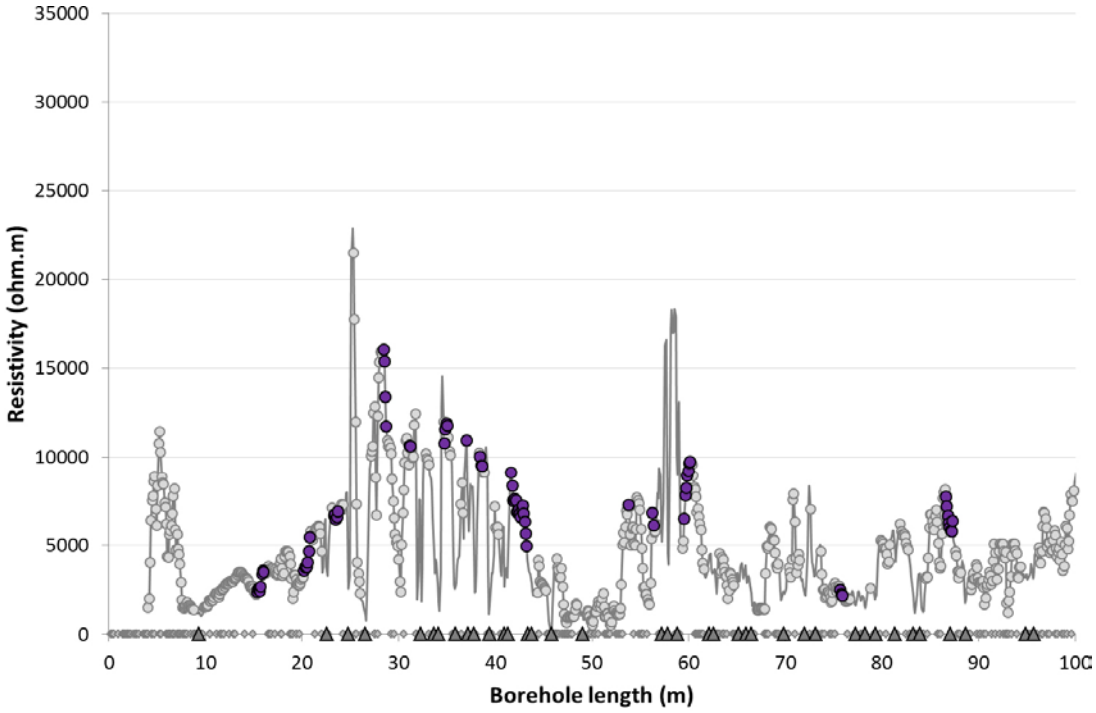

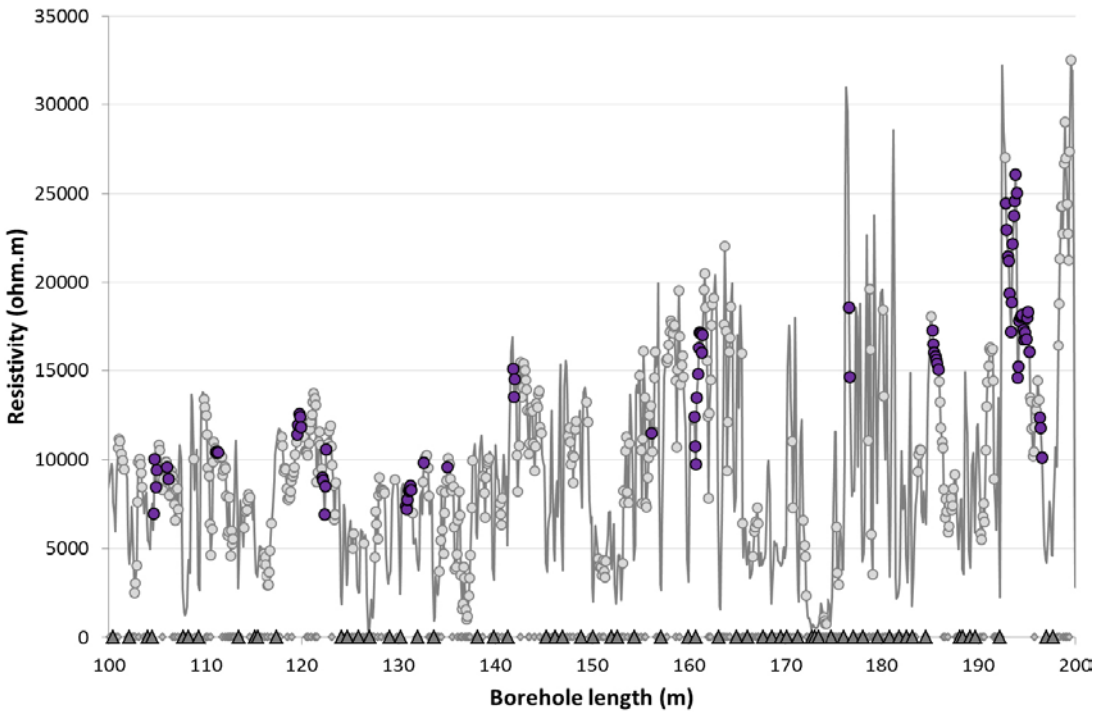

Rock resistivity
Fractured rock resistivity
Rock matrix resistivity
Location of interpreted open fracture
Location of hydraulically conductive fracture detected in the difference flow logging

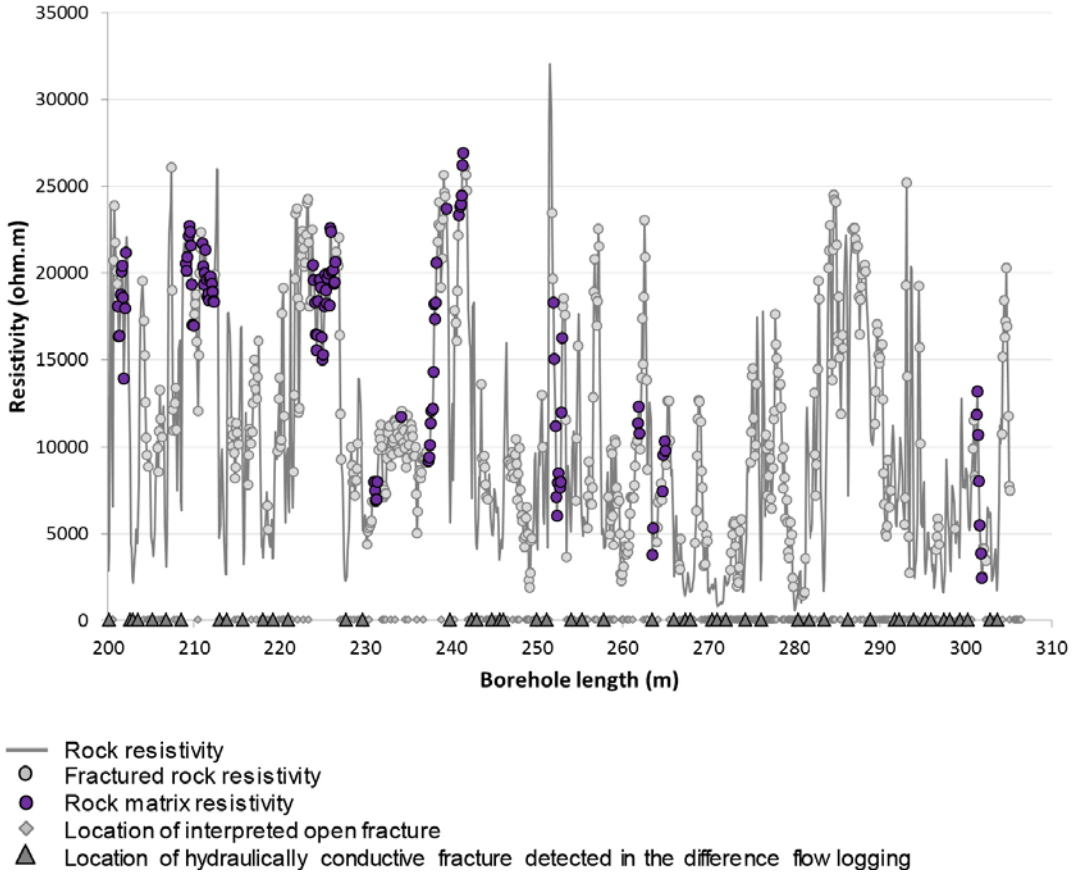
35000
30000
25000
20000
15000
10000
5000
0
Resistivity (ohm.m)
200
210
220
230
240
250
260
270
280
290
300
310
Borehole length (m)
Rock resistivity
Fractured rock resistivity
Rock matrix resistivity
Location of interpreted open fracture
Location of hydraulically conductive fracture detected in the difference flow logging

A2 In situ rock resistivities, open fractures, and flow anomalies KFR102B

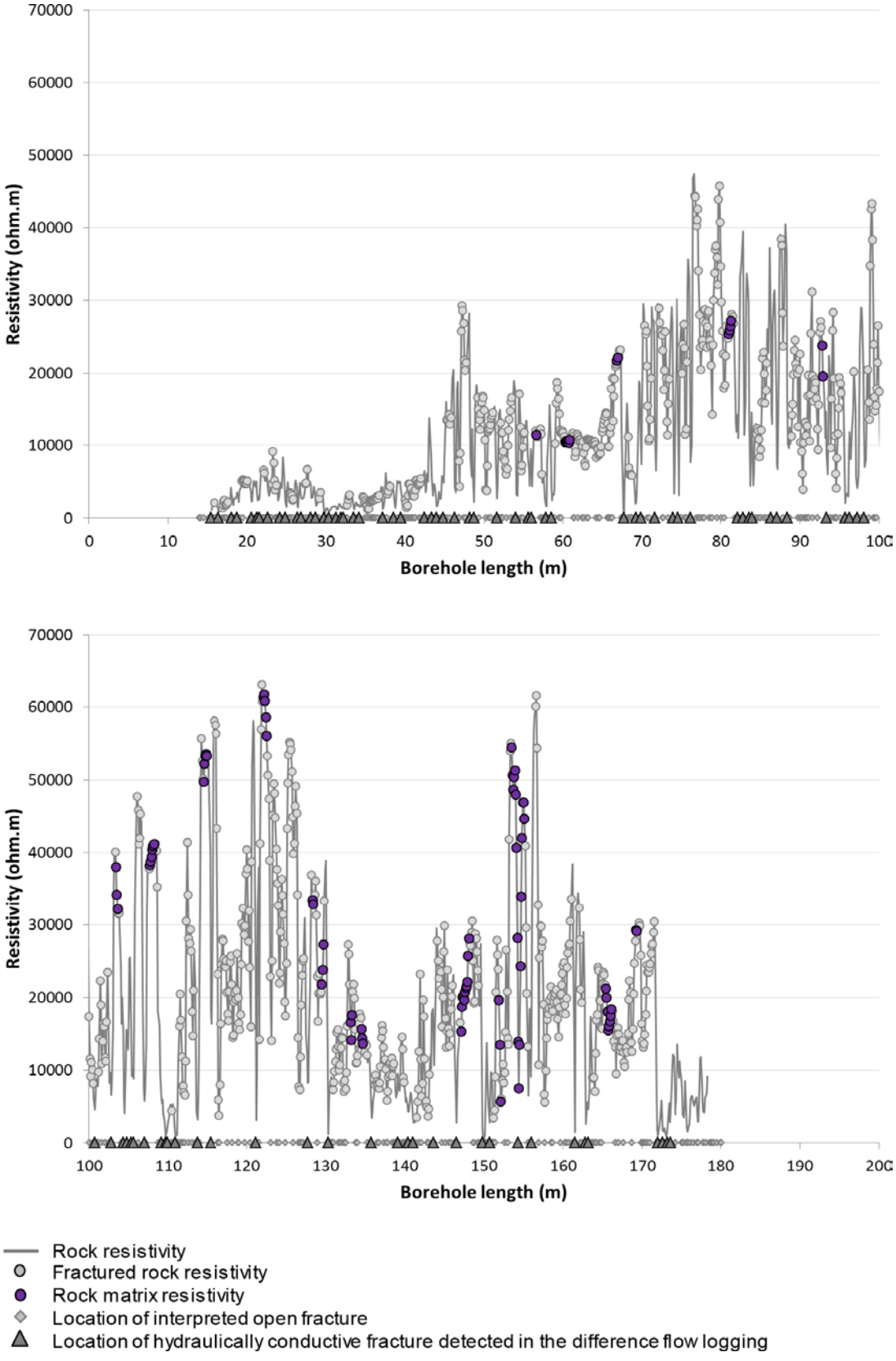

Appendix B

B1 Tabulated rock matrix resistivities KFR105

BH length (m)	Resistivity (ohm.m)	BH length (m)	Resistivity (ohm.m)	BH length (m)	Resistivity (ohm.m)
15.34	2402.21	42.74	7071.55	122.54	10554.7
15.44	2545.75	42.84	7264.84	130.74	7363.48
15.54	2541.71	42.94	6809.11	130.84	7206.89
15.64	2446.47	43.04	6350.56	130.94	7742.71
15.74	2692.07	43.14	5651.65	131.04	8259.54
15.84	3391.83	43.24	4962.89	131.14	8316.33
15.94	3592.37	53.74	7301.78	131.24	8516.33
16.04	3509.62	56.24	6838.55	131.34	8279.65
20.24	3578.57	56.34	6112.87	132.64	9835.45
20.34	3807.73	59.54	6501.3	135.04	9572.91
20.44	3758.68	59.64	7821.35	141.84	15094
20.54	3786.04	59.74	8234.98	141.94	13509.2
20.64	4031.01	59.84	8968.95	142.04	14501.3
20.74	4679.73	59.94	9190.89	156.14	11490.1
20.84	5452.59	60.04	9659.78	160.54	12401.7
23.34	6684.68	60.14	9744.43	160.64	10732
23.44	6743.34	75.74	2503.3	160.74	9719.14
23.54	6453.12	75.84	2269.1	160.84	13467.4
23.64	6564.63	75.94	2166.68	160.94	14805.9
23.74	6914.98	86.64	7752.27	161.04	16292.9
28.44	16032.3	86.74	7196.64	161.14	17180.2
28.54	15388.2	86.84	6662.65	161.24	17143.9
28.64	13405.2	86.94	6231.59	161.34	16027.5
28.74	11741	87.04	6017.23	161.44	17067.3
31.14	10638.3	87.14	5836.23	176.64	18583.1
31.24	10591.7	87.24	5807.31	176.74	14643
34.74	10793.1	87.34	6375.46	185.24	17310.5
34.84	11551.8	104.64	6970.13	185.34	16515.3
34.94	11915.9	104.74	10015.6	185.44	16009.1
35.04	11782.2	104.84	8434.59	185.54	15780.8
37.04	10954.5	104.94	9406.27	185.64	15606.4
38.44	10009.6	106.04	9555.25	185.74	15400.9
38.54	9548.84	106.14	8905.46	185.84	15061.3
38.64	9473.56	111.04	10415.2	192.84	24446.9
41.64	9122.79	111.14	10454.8	192.94	22945.6
41.74	8365.81	111.24	10420.6	193.04	21435.6
41.84	7523.58	119.54	11400.1	193.14	21211
41.94	7487.61	119.64	11948.3	193.24	19366.6
42.04	7621.53	119.74	12544.1	193.34	17192.8
42.14	7517.83	119.84	12389.7	193.44	18878.2
42.24	6857.16	119.94	11832.7	193.54	22167.9
42.34	6936.64	122.14	8993.67	193.64	23743.3
42.44	7048.92	122.24	8813.93	193.74	24578.6
42.54	6770.34	122.34	6905.08	193.84	26048.1
42.64	6573.34	122.44	8487.08	193.94	25035.6
194.04	14616.6	211.84	19675.2	237.94	14289.8
194.14	15230.4	211.94	19805.7	238.04	18220.8
194.24	17820	212.04	19369.5	238.14	17339.7
194.34	18034.6	212.14	18917.4	238.24	18313.4
194.44	18120	212.24	18377.2	238.34	20556.6
194.54	18170.5	212.34	18349.7	239.44	23695

BH length (m)	Resistivity (ohm.m)	BH length (m)	Resistivity (ohm.m)	BH length (m)	Resistivity (ohm.m)
194.64	17336.8	223.94	20435.5	240.94	23308.3
194.74	16766.4	224.04	19581.7	241.04	23836.4
194.84	17152.7	224.14	18290.6	241.14	23927.8
194.94	16777.1	224.24	16471.4	241.24	24451.1
195.04	17991	224.34	15536.3	241.34	26209.6
195.14	18333.9	224.44	16425.1	241.44	26947.9
195.24	16052.7	224.54	18363.3	251.94	18311.4
196.34	12370.9	224.64	19564.7	252.04	15050.4
196.44	11786.1	224.74	19625.8	252.14	11187.1
196.54	10119.1	224.84	19176.1	252.24	7123.53
201.14	18098.2	224.94	16284.9	252.34	6061.52
201.24	16334	225.04	15023.4	252.44	7942.89
201.34	16399.8	225.14	15285.2	252.54	8503.13
201.44	18761.3	225.24	18065.5	252.64	7663.36
201.54	20064.7	225.34	19923.2	252.74	8007.67
201.64	20408.9	225.44	19010.9	252.84	11976.2
201.74	18579.2	225.54	18231.7	252.94	16275.4
201.84	13933	225.64	19718.9	261.74	11368.6
201.94	17968	225.74	19974.3	261.84	12314.8
202.04	21159.2	225.84	18145.8	261.94	10768.4
209.04	20530.5	225.94	22553.6	263.44	3769.13
209.14	20140.3	226.04	22379.9	263.54	5352.16
209.24	20907.4	226.14	20071.7	264.64	7461.27
209.34	22117.8	226.24	20177.9	264.74	9544.69
209.44	22693.8	226.34	19371.1	264.84	10324.6
209.54	22376.6	226.44	19447.9	264.94	9786.74
209.64	21590.5	226.54	20613.7	301.24	11850.9
209.74	19314.5	231.04	8003.13	301.34	13190.4
209.84	16993.1	231.14	7504.8	301.44	10685.1
209.94	16983.8	231.24	6913.26	301.54	8029.36
210.94	21706.9	231.34	7015.75	301.64	5490.39
211.04	20371	231.44	8011.86	301.74	3832.1
211.14	19336.6	234.14	11735.1	301.84	2410.06
211.24	20009	237.34	9187.39		
211.34	21316.6	237.44	9415.3		
211.44	19615.5	237.54	10109		
211.54	18635.7	237.64	11348.3		
211.64	18785.6	237.74	12073.3		
211.74	18412.6	237.84	12190.7		

BH length = Borehole length

B2 Tabulated rock matrix resistivities KFR102B

BH length (m)	Resistivity (ohm.m)	BH length (m)	Resistivity (ohm.m)	BH length (m)	Resistivity (ohm.m)
56.60	11418	122.20	61742.5	153.60	50658.8
60.30	10418.6	122.30	60872	153.70	48606.4
60.40	10512.1	122.40	58605.9	153.80	50381.4
60.50	10621.6	122.50	56045.6	153.90	51260.9
60.60	10583.1	128.30	33395.8	154.00	47965.2
60.70	10316.9	128.40	32863.2	154.10	40623
60.80	10715.3	129.50	21794	154.20	28227.6
66.80	21707.8	129.60	23760.6	154.30	13937
66.90	22173.1	129.70	27273.5	154.40	7488.62
81.00	25385.4	133.10	16540.7	154.50	13515.2
81.10	25899.2	133.20	14163.8	154.60	24301.4
81.20	26481.2	133.30	17559	154.70	33928.3
81.30	27175.1	134.50	15678.2	154.80	41984.6
92.80	23768.1	134.60	14367.4	154.90	46851.6
92.90	19596.7	134.70	13682.7	155.00	46844.5
103.40	38013.3	147.10	15296.1	155.10	44620.7
103.50	34181.5	147.20	18739	165.40	21209.9
103.60	32167.2	147.30	20054.1	165.50	19976.7
107.70	38236.1	147.40	20272.9	165.60	18080.5
107.80	38764.9	147.50	19645.2	165.70	15472.9
107.90	39421	147.60	20721.7	165.80	16099
108.00	40419.4	147.70	21293.6	165.90	16753.4
108.10	40941.3	147.80	21591	166.00	17474.5
108.20	41117.1	147.90	22136	166.10	18387.2
114.50	49683.3	148.00	25737	169.20	29284.8
114.60	52176.8	148.10	28097.6	169.30	29101.3
114.70	53300	151.90	19649.9		
114.80	53560.3	152.00	13488.8		
114.90	53322	152.10	5648.12		
122.10	61308.6	153.50	54452.6		

BH length = Borehole length

Appendix C

C1 In situ formation factors KFR105

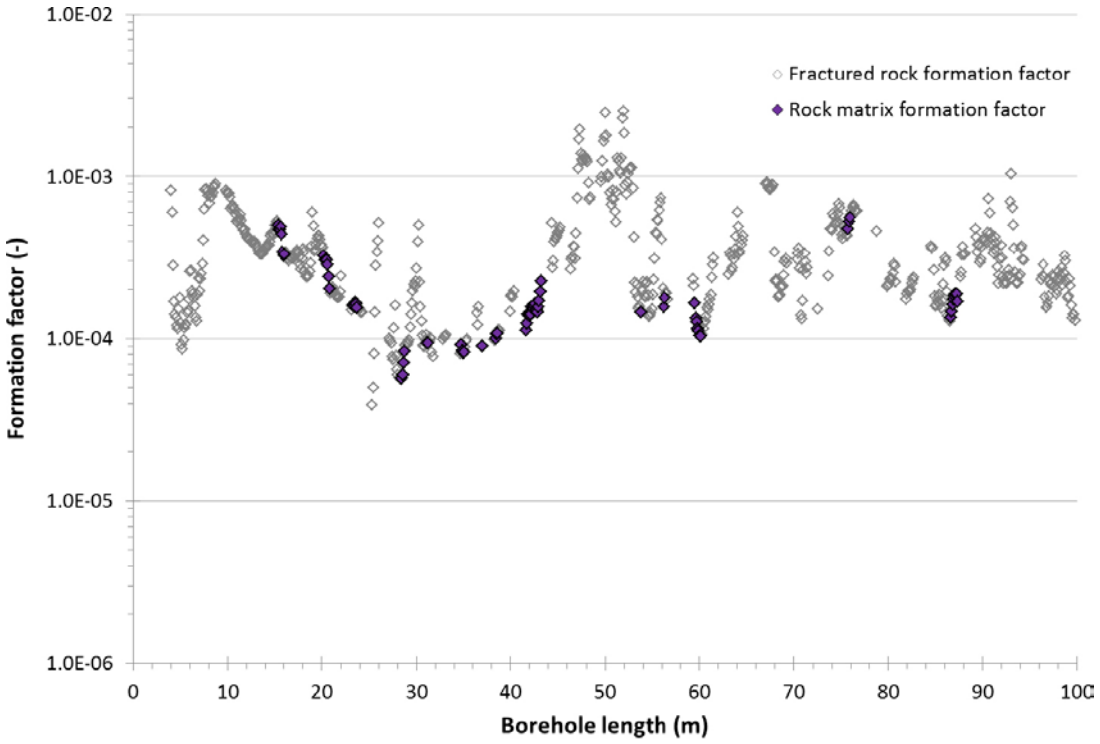

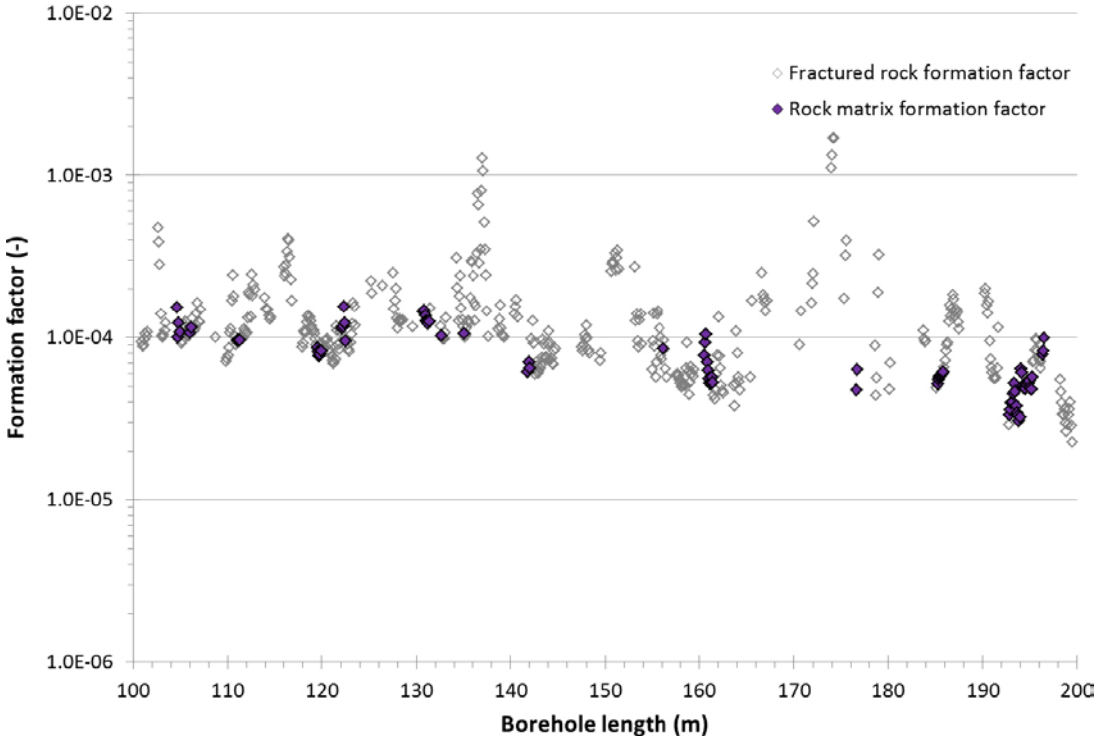

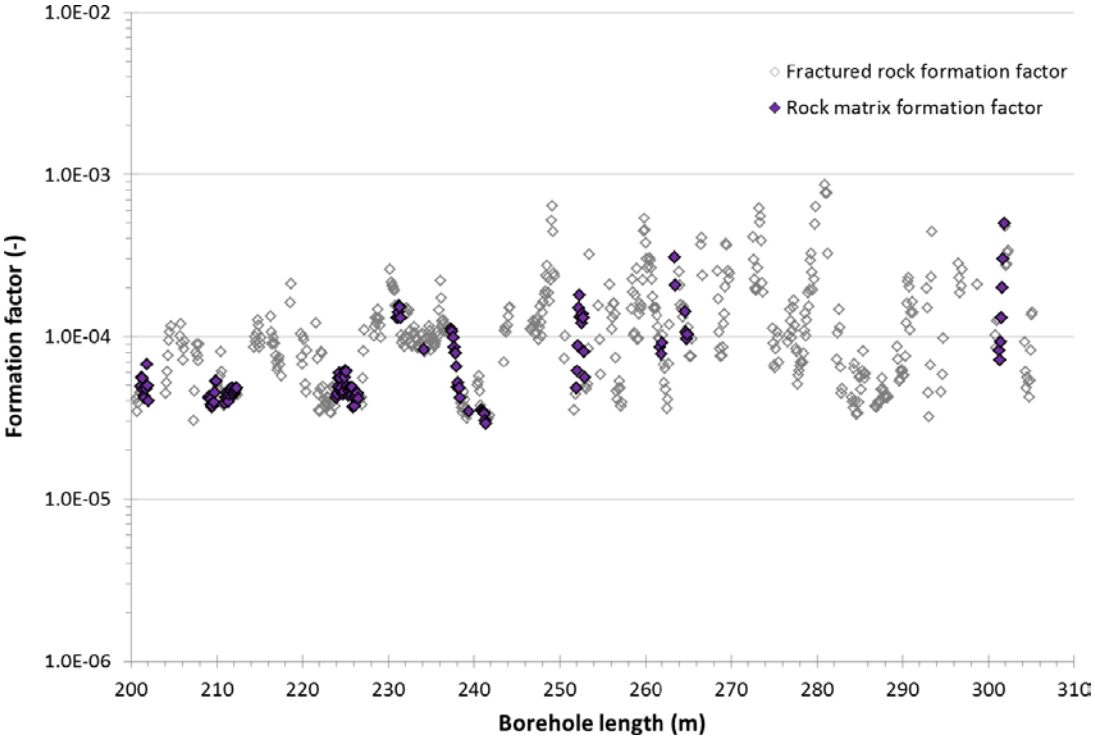
1.0E-02
1.0E-03
1.0E-04
1.0E-05
1.0E-06
Formation factor (-)
200
210
220
230
240
250
260
270
280
290
300
Borehole length (m)
Fractured rock formation factor
Rock matrix formation factor

C2 In situ formation factors KFR102B

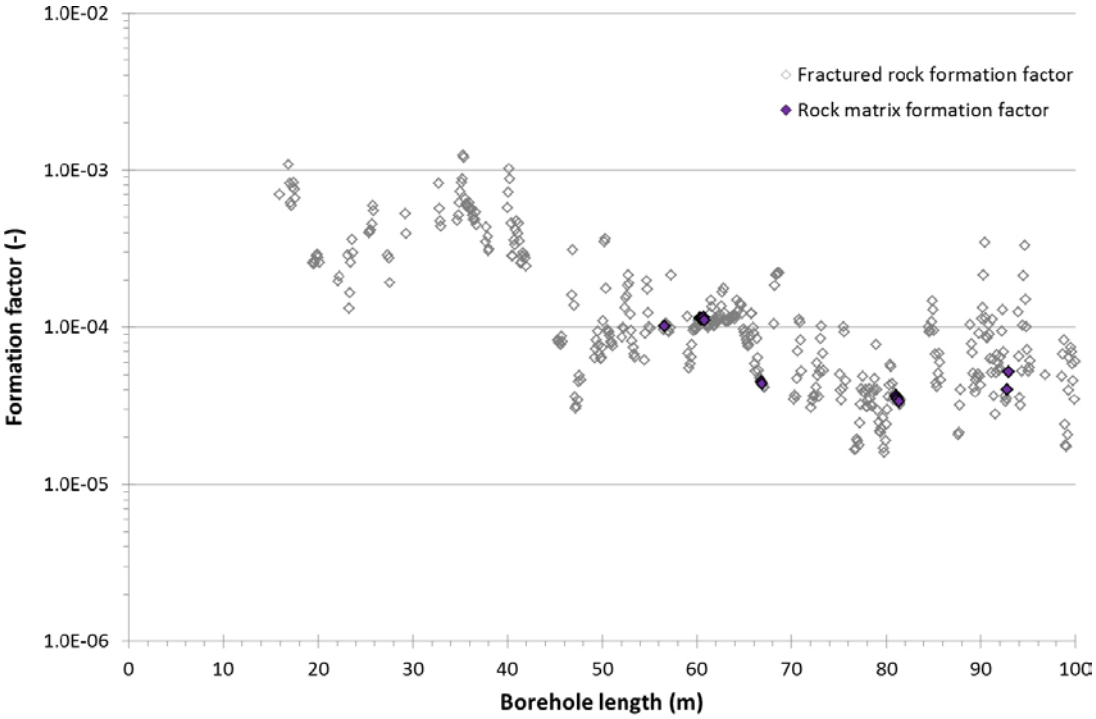

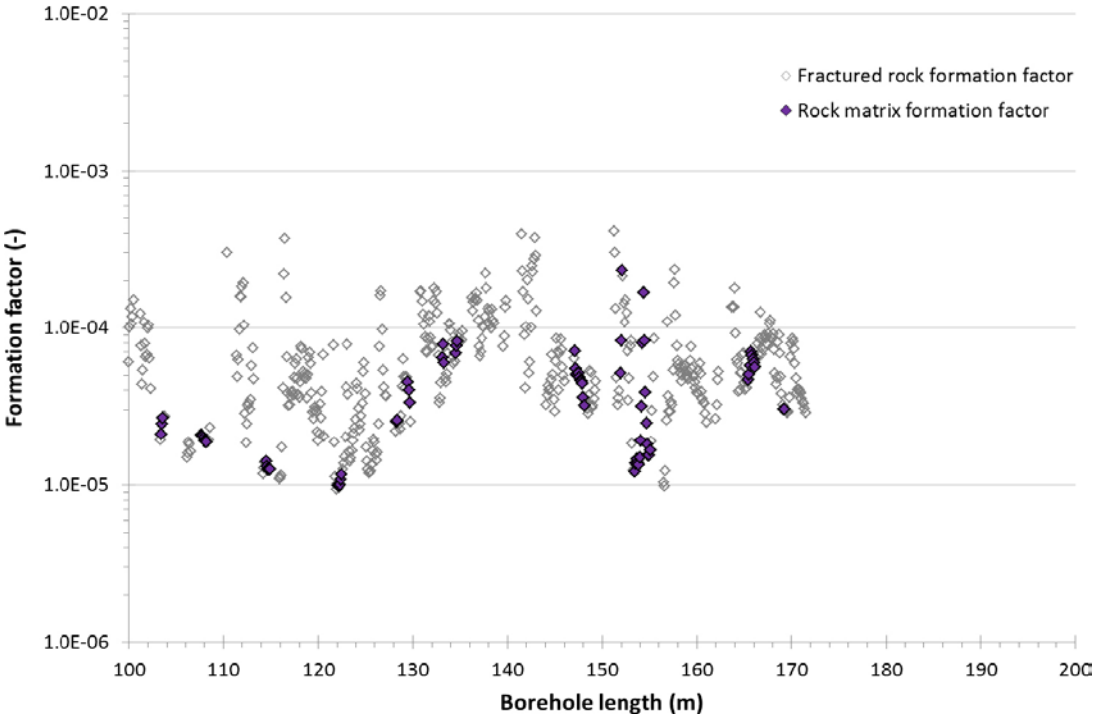

Appendix D

D1 Histograms of apparent formation factors KFR105

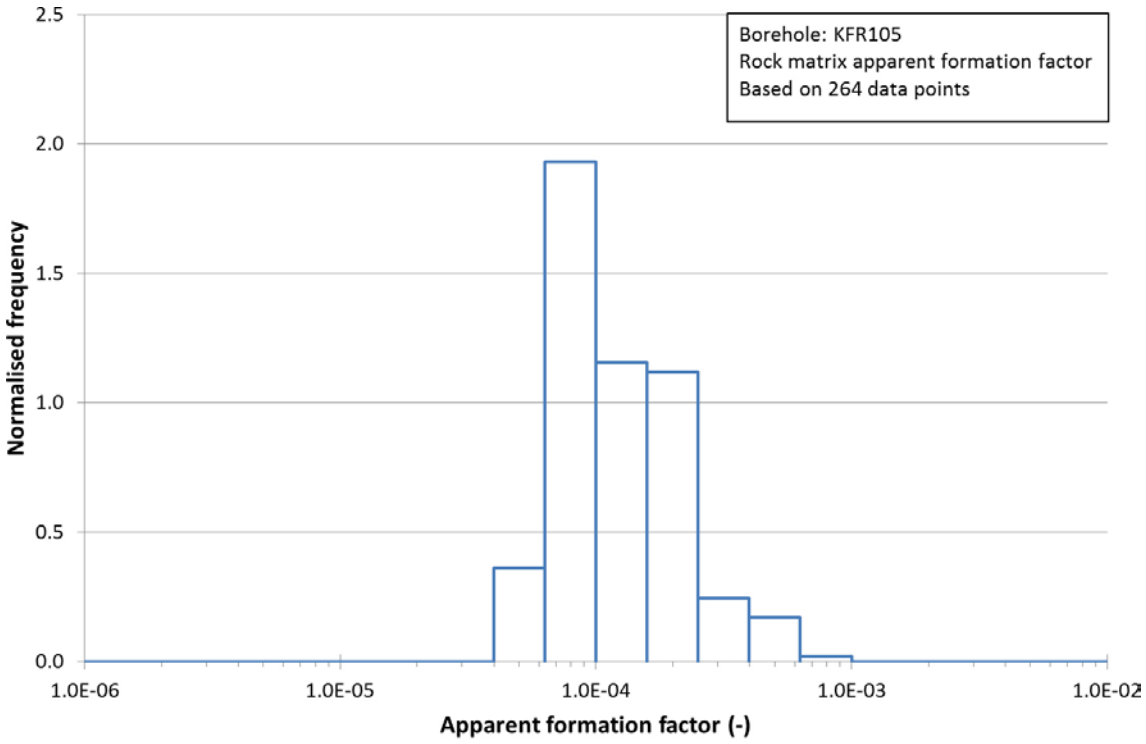

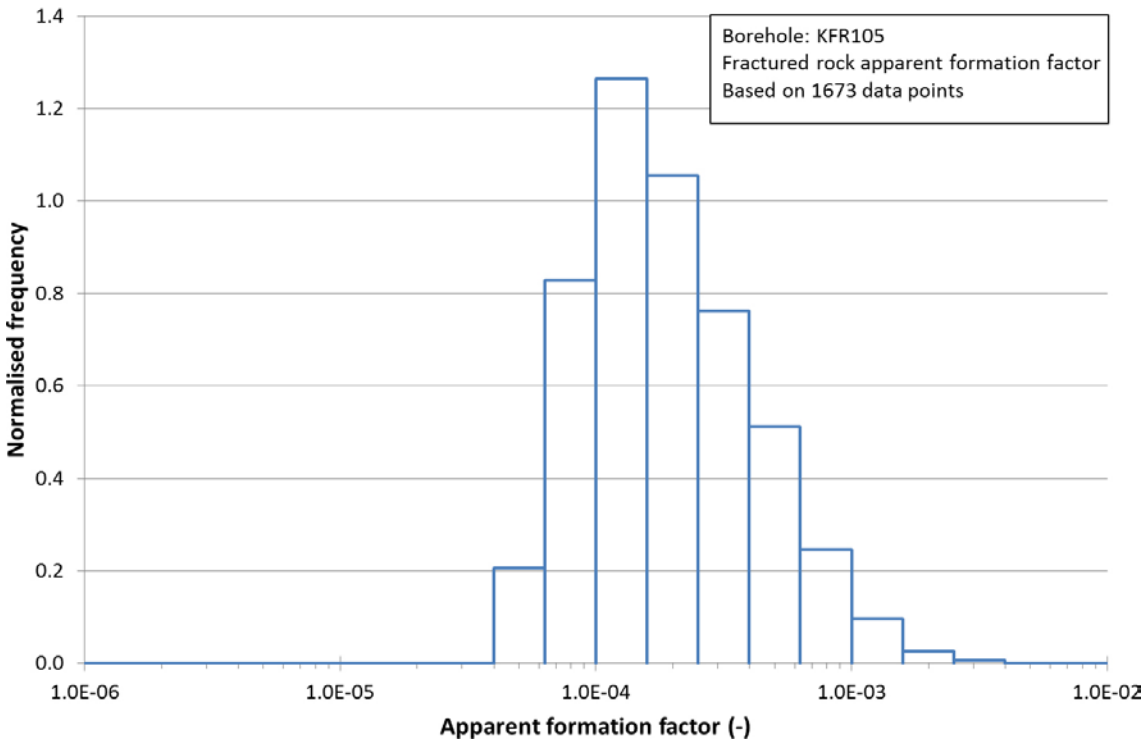

D2 Histograms of apparent formation factors KFR102B